CLRC

Technical Report
RAL-TR-97-018

ROTAX 95/96
Activity Report

W Kockelmann H Tietze-Jaensch E Jansen and W Schäfer

April 1997

COUNCIL FOR THE CENTRAL LABORATORY OF THE RESEARCH COUNCILS

Enquiries about copyright, reproduction and requests for additional copies of this report should be addressed to:

The Central Laboratory of the Research Councils
Library and Information Services
Rutherford Appleton Laboratory
Chilton
Didcot
Oxfordshire
OX11 0QX
Tel: 01235 445384 Fax: 01235 446403
E-mail library@rl.ac.uk

ISSN 1358-6254

ROTAX 95 / 96: Activity Report

W. Kockelmann[1,2], H. Tietze-Jaensch[1,2], E. Jansen[1] and W. Schäfer[1]

[1)] Mineralogisch-Petrologisches Institut, University of Bonn, Poppelsdorfer Schloss, D-53115 BONN, Germany

[2)] ROTAX, Rutherford Appleton Laboratory, ISIS Facility, Chilton, Didcot, OX11 0QX, UK

This report reflects the major activities of the ROTAX team in the years 1995 and 1996. It has been a difficult transition period of converting ROTAX from a time-of-flight spectrometer development machine into a user-scheduled operational instrument for multi-purpose conventional time-of-flight diffraction. However, we believe it has been a successful one and look forward very much to welcoming old and new users to perform their experiments on ROTAX. After all, ROTAX remains the only German-owned neutron scattering instrument based at ISIS, today's most powerful pulsed spallation neutron source. Thus, ROTAX is important for the international scientific collaboration between the United Kingdom and Germany. Even more so as we believe that spallation neutron sources own the future in neutron scattering and should be further exploited for research in science and scientific education.

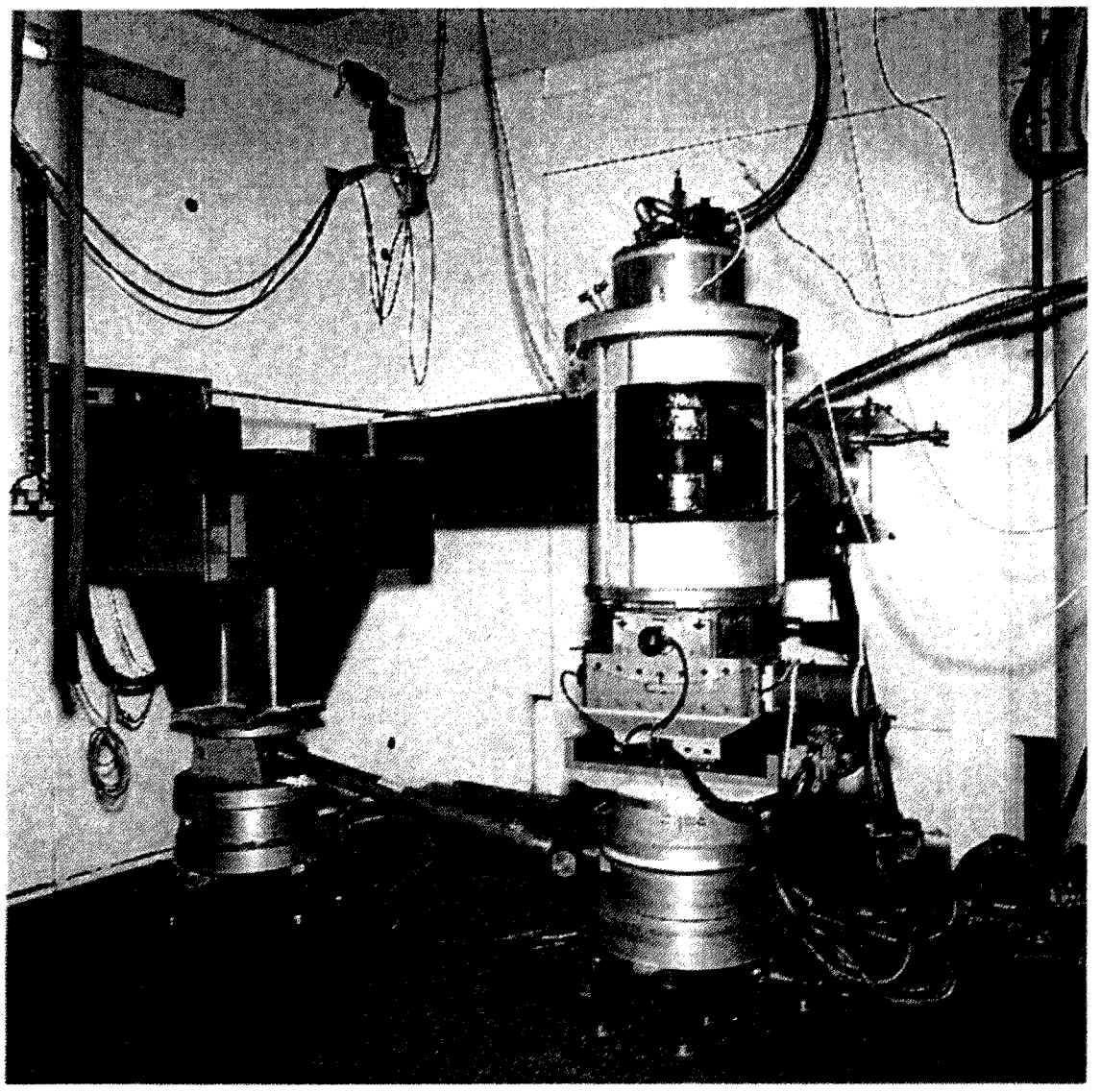

View of the ROTAX / DIFF neutron time-of-flight diffractometer

Contents:

Appendix:

Word V6.0 templates of the ROTAX beam time application form and the ROTAX experimental report form can be downloaded from the ROTAXA::ANONYM account using FTP to: IP-addresss *130.246.48.68;* login *ANONYM;* subdirectory *[.FORMS];* files RTX_C.DOC (beam time application form), RTX_EXRA.DOC (experimental report form).
Other files of general interest can be downloaded from subdirectory *[.RTX_DOCS].*

1. Time of Flight Diffractometer ROTAX / DIFF

1.1 Layout of the Instrument

ROTAX is located on the N2 beam at ISIS behind the PRISMA spectrometer viewing the cold (95K) poisoned methane moderator on a 14-16 metre variable length in-pile beam-tube. The sample table is equipped with triple-axis like rotational stages and a $\pm 20^\circ$ double-goniometer, all made of non-magnetic material. The ROTAX sample table takes any ISIS sample environment kit and can carry up to 500 kg load. The detectors swivel on air pads and are mutually attached to the 2Θ (A4) rotational drive at variable distances between 0.5 and 1.6 meteres for the scattered flight path. All angles are remotely controlled and encoded using absolute decoders. The schematic layout of ROTAX is sketched in Fig. 1.1 and the instrument parameters are given in Tab 1.1.

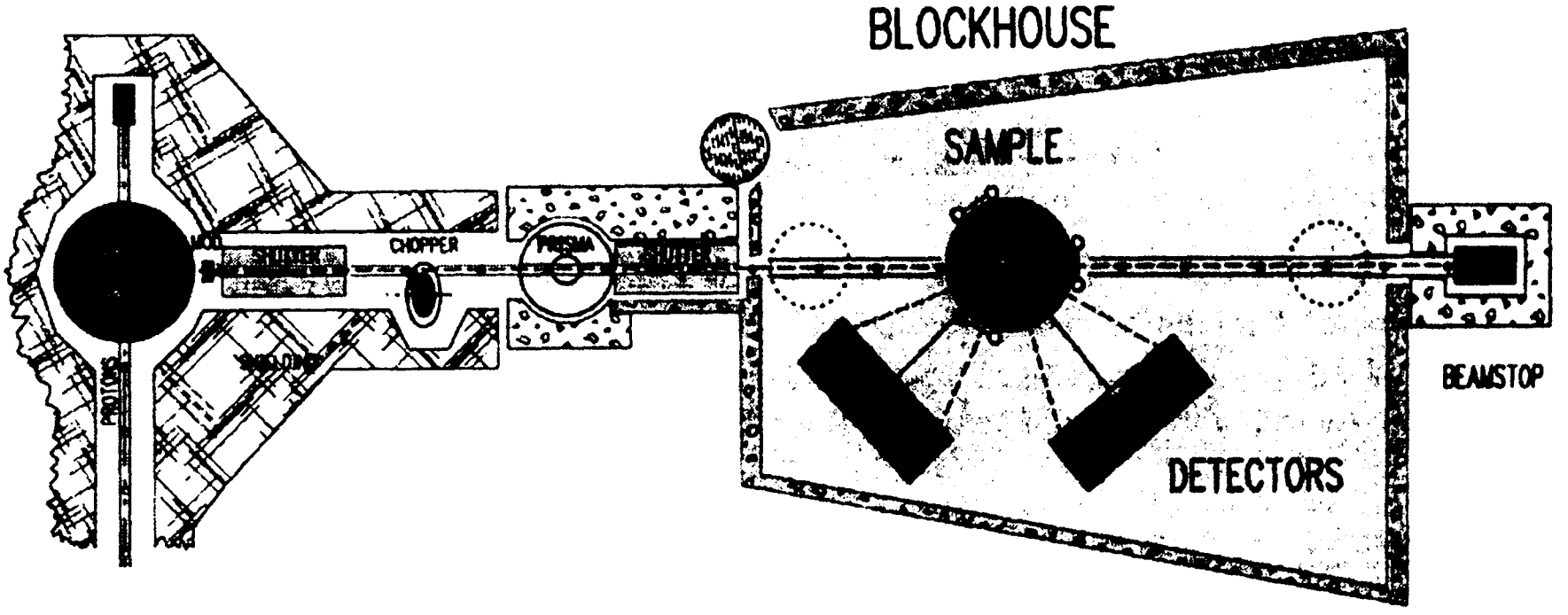

Fig. 1.1: Schematic diagram of the ROTAX / DIFF neutron time-of-flight diffractometer

Tab 1.1: ROTAX / DIFF instrument parameters

d-range	0.3 - 50	[Å]
resolution $\Delta d/d$	$4 \cdot 10^{-3}$	
flux at sample	$1 \cdot 10^{6}$	[n/s cm^2]
incident ToF path	14.0 - 16.0	[m]
scattered ToF path	0.5 - 1.6	[m]
total ToF length	14.5 - 17.6	[m]
scattering angle	3 - 175	[deg]
incident energy	3 - 450	[meV]
incident wavelength	0.4 - 5.0	[Å]
time window	1 - 20	[ms]
detector resolution:		
position Δr	2.5	[mm]
time Δt	1.0	[µsec]

1.2 Time-of-Flight Diffraction at ROTAX

The metric information contained in diffraction patterns is interpreted in terms of the Bragg equation:

$$2\, d_{hkl}\, sin\, \Theta = \lambda \qquad (1.1)$$

d_{hkl} is the d-spacing of a particular reflection, θ is half the scattering angle, λ the (neutron)-wavelength.

On a reactor neutron source, diffraction is usually performed on a monochromatic beam-line and diffraction data are collected in an angle-dispersive mode. A diffraction pattern is, therefore, plotted as intensity vs. scattering angle 2Θ. In contrast, neutron time-of-flight diffraction takes advantage of the finite velocity of thermal neutrons which is linked to the wavelength by de Broglie's relation.

$$\hbar k = h/\lambda = m_n v = m_n L / t \qquad (1.2),$$

with m_n the neutron mass, h resp. $\hbar$ Planck's constant, v neutron velocity, $L=L_i+L_f$ total flight path, t total time-of-flight (on ROTAX the time frmae is usually binned to 2^{12} channels). Combining eqs. (1.1) and (1.2) yields the tof-Bragg equation:

$$t = \frac{Lm_n}{h}\lambda = \frac{2m_n}{h} L d_{hkl} \sin\Theta \qquad (1.3)$$

From this key-equation it is immediately obvious that a tof-diffraction pattern appears as a set of straight lines when t is plotted versus sin Θ, their linear slopes being proportional to d_{hkl} (see Fig. 1.2). A plot of $t(d_{hkl})$ vs. the instrument variable 2Θ illustrates how the d-range can be altered very easily simply by varying the angular setting of the multi-counter detector (Fig. 1.3).

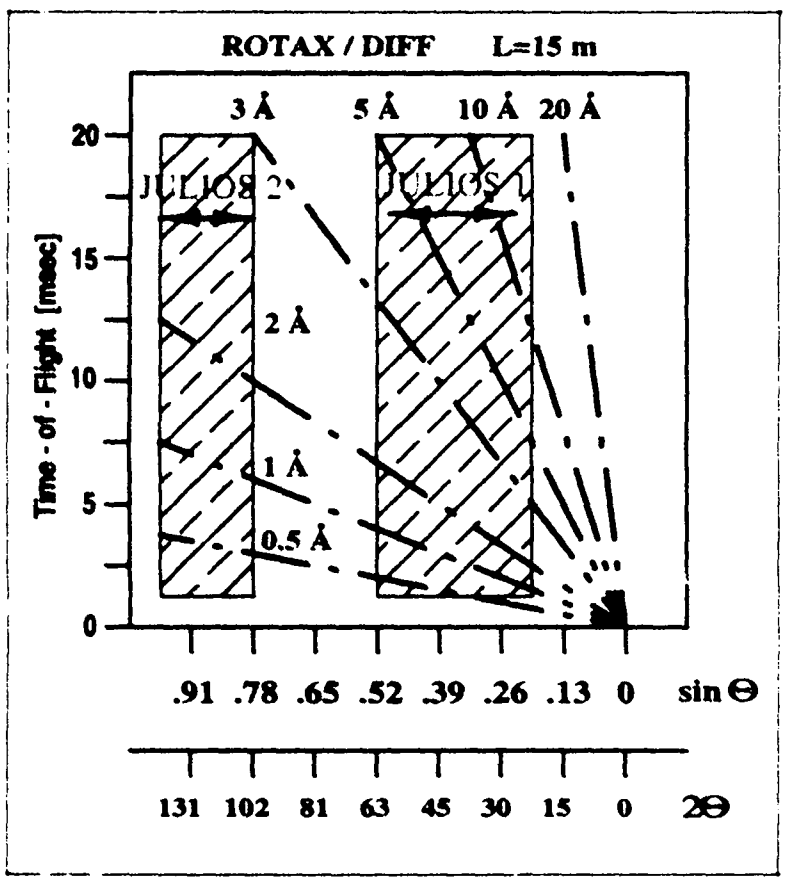

Fig. 1.2: *d-range in time-of-flight vs. sinΘ which is covered simultaneously by a tof-diffractometer equipped with a position sensitive detector of a certain length L_D. The direction of the abscissa is inversed because of the actual (negative) scattering sense on ROTAX.*

To first order the $\Delta d/d$ resolution function is obtained by differentiating eq. (1.3):

$$\frac{\Delta d}{d} = \sqrt{\left(\frac{\Delta t}{t}\right)^2 + \left(\frac{\Delta L}{L}\right)^2 + \left(\Delta\Theta ctg\Theta\right)^2} \qquad (1.4).$$

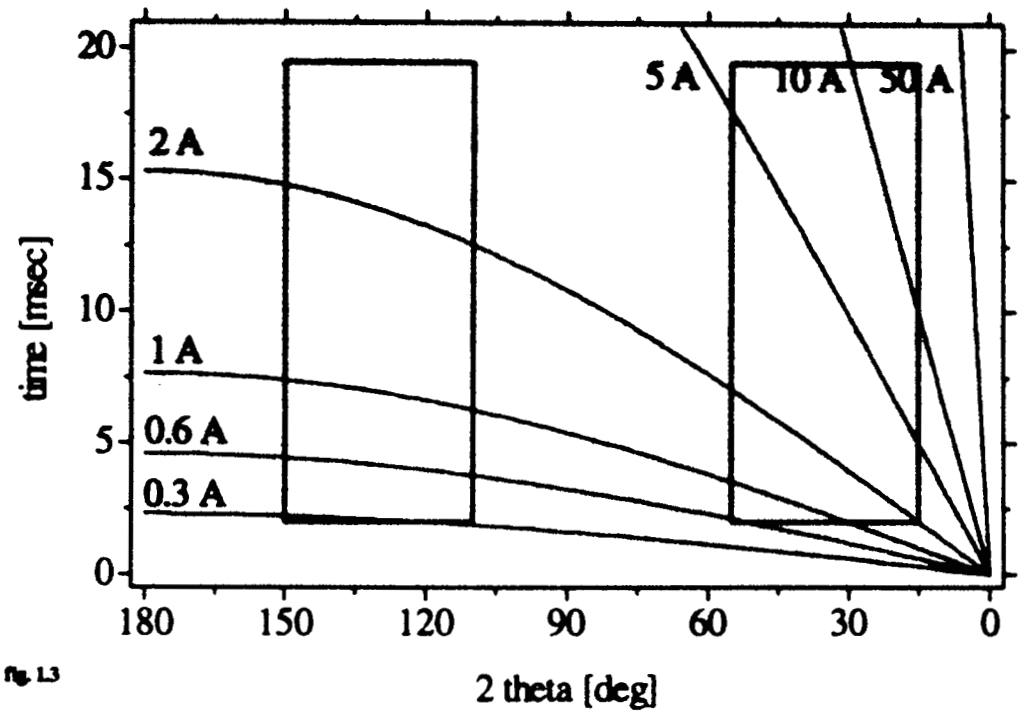

Fig. 1.3: Time-of-flight - 2Θ parameter window on ROTAX in its standard setting with 2 JULIOS detectors (indicated by the boxes).

On ROTAX the uncertainties are of the order of $\Delta t \approx 30\ \mu s$, $\Delta L \approx 3.5$ cm and $\Delta\theta \approx 0.07°$ (Fig. 1.4). The time uncertainty Δt is itself neutron energy dependent. Therefore, only an average value is given which depends much on the moderator type, i.e. the time decay constant of the neutron pulses from the warmer ambient water moderator is 30% shorter than those from the 95K methane moderator. That is why the best resolution ever achieved on ROTAX ($\Delta d/d \approx 2.8\ 10^{-3}$) was at the time when water temporarily replaced the methane moderator. For small values of d_{hkl} the resolution function eq. (1.4) is approximately constant.

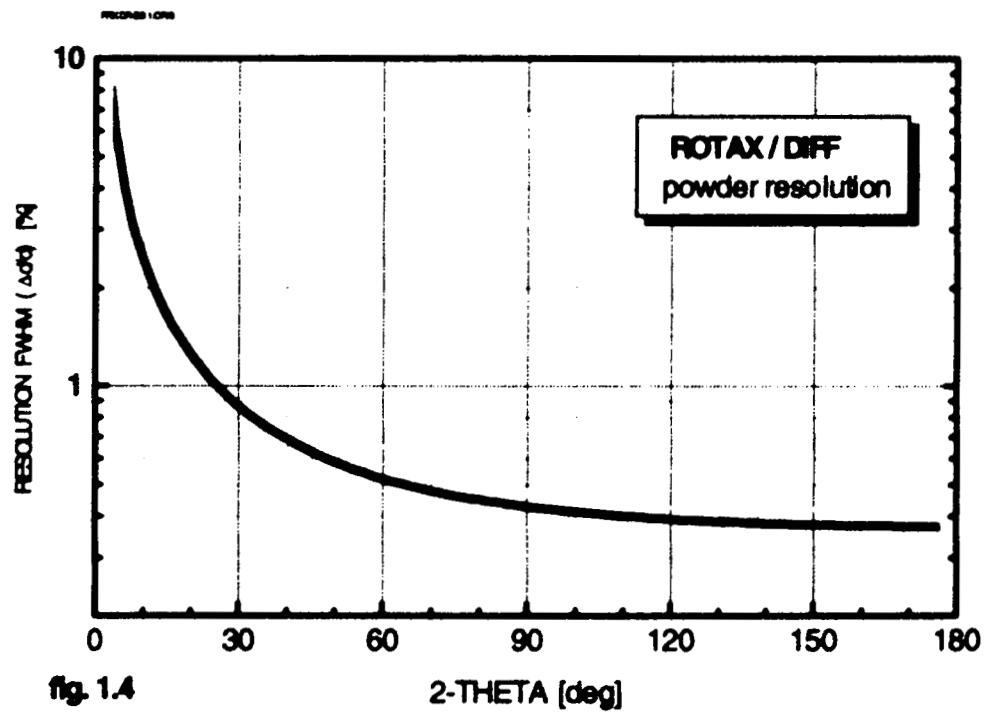

Fig. 1.4: First order resolution function Δd/d for ROTAX in standard set-up.

The asymmetric moderator time decay function is responsible for the typical time-of-flight peak asymmetry [1-3] in the tof-diffraction patterns which must be taken into account with all subsequent data analysis software.

Looking at eq. (1.3) the advantages of tof-diffraction are immediately obvious:

1. Tof-diffraction is possible on a white incident beam and all incoming neutrons of different energies respectively wavelengths can be used. This results in an enormous increase of the accessible range of momentum transfer Q or d-spacing, respectively.

2. The full information of a diffraction pattern is obtained at a single constant scattering angle. This can be very important when the use of specific sample equipment imposes limitations on the scattering angles (e.g. the use of a pressure cell or magnet).

3. A huge multiplex advantage of typically two orders of magnitude is achieved by using all incoming neutron energies simultaneously, i.e. if a diffraction pattern is acquired with multi-detectors covering a large range of scattering angles.

4. The resolution function is almost constant, particularly in the range of increasing peak overlap.

Taking into consideration the geometry of the two individually operated linear position sensitive JULIOS detectors (Fig 1.5), the Bragg angle θ as a function of each detector position channel x reads:

$$2\theta(x) = 2\theta_0(x_0) + \tan^{-1}\left(\frac{x_0 - x}{L_{f0}}\frac{L_D}{N_x}\right) \qquad (1.5),$$

with x_0 the centre-channel of the detector, L_D its active length, L_{f0} its centre distance from the sample and N_x the number of position channels; usually N_x=256. Equations 1.3 and 1.5 unambiguously identify a particular d-spacing value to every individual pixel in the (t,x) raw data pattern.

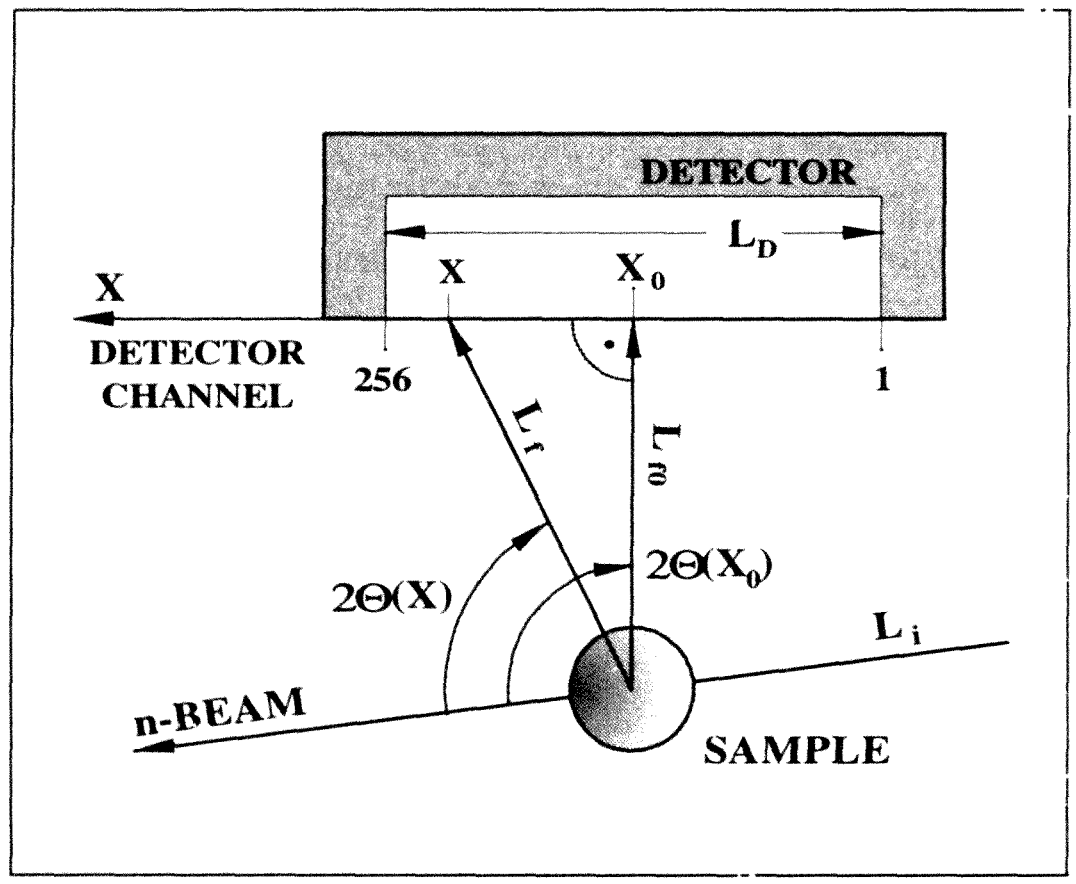

Fig. 1.5: Scattering geometry of the JULIOS detector

The raw data intensities obtained need to be normalised to the energy / time dependent incoming neutron flux. This procedure is commonly known as the so-called focussing where an integration or constant d-value histogramming of the original 2-dimensional d-value matrix is performed. An example of this procedure is illustrated in Fig. 1.6. The 2-dimensional raw data spectrum (Fig. 1.6a) which, if integrated, would yield an unnormalised powder diffraction pattern (Fig. 1.6 b), is divided by the monitor spectrum (Fig 1.6 c), which is gauged against a vanadium spectrum and automatically corrects for the incoming neutron flux and the individual position channel efficiency values of the detectors. The result is plotted in Fig 1.6 e for the 2-dim. (t,x) data representation. After line-integration along the powder lines of constant d-values the result is a tof-powder diffraction pattern of intensities plotted vs. d-spacing (Fig. 1.6 f), ready for any further profile refinement procedure.

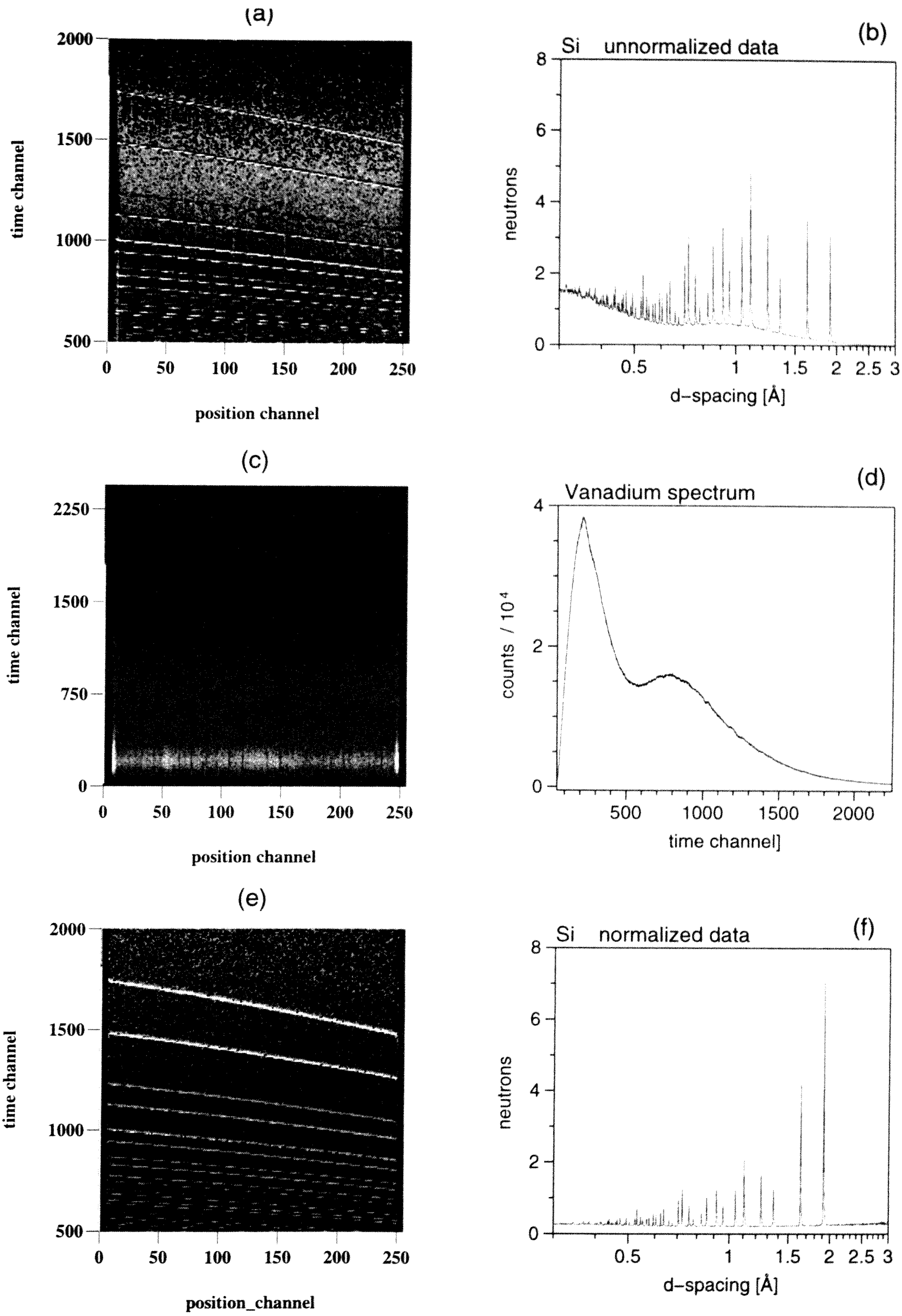

Fig 1.6: *Raw data normalisation on ROTAX: (a) raw data (t,x) pixel pattern and (b) integrated along constant d-value pixels; (c) monitor / vanadium spectrum and (d) time-channel / wavelength intregrated; (e) normalised data (t,x) pixel pattern ((a) / (c)) and (f) integrated along constant d-value pixels.*

2. Science on ROTAX in 1995 and 1996

During the two years of routine operation ROTAX was used as a time-of-flight diffractometer mainly for powder samples. The UK and German shares of available beam time were approximately equal (see Fig 4.1). About 11% was used for instrument time, such as installation and calibration of new components, maintenance or repair time. A total of 37 scientific projects (Tab. 2.1 at the end of this chapter) with 121 individual experiments were performed. The diversity of the science on ROTAX can be classified into a (still increasing) block of magnetism (27%) and an equally large number of projects dealing with the localisation of light elements (H, D, N) (27%). The study of structural and orientational disorder (19%) in solids was at third rank followed by 14% for general crystal structure determination and refinement (see Fig. 2.1). Not included in these statistics are the texture measurements because these projects were at the stage of developement (see chapter 3.2.1) and details are reported elsewhere [4-5]. However, gathering pole-figures by the time-of-flight technique appears to be very promising and achieves real experimental gain factors of 5-10 by simultaneous multiplexing of the incident white beam.

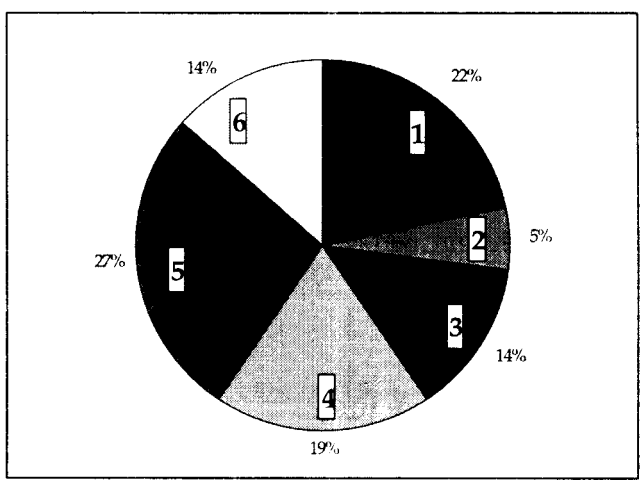

Fig 2.1: Diversity of scientific projects performed on ROTAX in 1995/96:

1: magnetic structure determination
2: other magnetism studies
3: crystal structure refinement
4: disorder problems
5: light element (H,D,N) localisation
6: site occupancy determination

Some highlights of the various projects are outlined here:

The main application in powder diffraction was nuclear and magnetic structure determination and structure refinement with respect to special questions, such as site occupancy, light element localisation or orientational disorder.

- Structure determination of iron nitrides of varying composition by D. Rechenbach and H. Jacobs (U. Dortmund). These materials are of fundamental importance for steel production and hardening. In particular the N site occupancies and thermal vibrational amplitudes were studied and determined.
- Orientational disorder and some dynamic properties of the amide ion in KNH_2/KND_2 were scrutinised by a joint group from U. Kiel and U. Dortmund (M. Müller, W. Press, J. Senker, H. Jacobs). This compound undergoes phase transitions triggered by varying anisotropic thermal vibrations of the amide molecule. Likewise the anisotropic orientational disorder in perovskite-related structures was studied (C. Eilbracht, H. Jacobs; U. Dortmund).
- There was a number of other projects of light element (H, D, N) localisation and site determination in various compounds. For details refer to the experimental reports (appendix A4).

- Site exchange of rare earth intermetallic compounds was the agenda of O. Moze (U. Parma, Italy). Further, valence fluctuations in some Ni-cuprates as well as structural and magnetic properties of La-Fe-Al-N and Tb-Co-Ga compounds were investigated with great success.
- Investigating the incommensurate sinusoidal structure of the ferro/antiferromagnetic mixed system $Tb(Ni,Co)C_2$ continued in a successful cooperation of J. Yakinthos (U. Thrace, Greece) and our own group.
- A number of projects dealt with magnetic structure determinations, e.g. $NaFeGe_2O_6$ for M. Behruzi (RWTH Aachen) or $CeRh_2Si_2/CeNi_2Ge_2$ (C. Frost; ISIS) or $Y(Co,Mn)_2Si_2$ by M. Hofmann (ISIS and HMI Berlin).
- Cation distributions were the purpose of two projects, one on a spinel type compound $Zn_{0.5}LiTi_{1.5}O_4$ (W. Potzel; TU München, E. Rönsch; TU Dresden; W. Schäfer, U. Bonn); the other one on Co-Mg mixed olivines by R. Hock (U. Würzburg) and A. Kirfel (U. Bonn).

Further, there were two single crystal projects:

- Spin fluctuations and diffuse magnetic scattering in the laves phase of $HoCo_2$ that is triggered by a collapse of the spin-wave excitation energies close to the first order ferri-magnetic phase transition. This is a joint project of P. Fabi (ISIS), E. Gratz (TU Wien), W. Schmidt (ILL Grenoble) and H. Tietze-Jaensch (ISIS).
- The field/temperature magnetic phase diagram was refined and the magnetic domain volume distribution was determined in the 2-dimensional magnetic system Rb_2MnCl_4. This project is part of an extended collaboration with R. v d Kamp and M. Steiner (HMI Berlin), W. Schmidt (ILL Grenoble), W. Treutmann (U. Marburg), R. Geick (U. Würzburg) and ourselves.

New methods will be exploited in addition to on-going instrument improvement in order to widen the scientific base and applicability of ROTAX. Another important aspect will be the training of post-graduate and post-doc students with time-of-flight neutron scattering methods.

Tab. 2.1: *Scientific projects on ROTAX in 1995/1996*

substance	**applicant**	**topic**
$CeNi_3Cu_3$ $CeNi_4Cu_2$	O. Moze (Physics, U Parma)	site occupation
$CeRh_2Si_2$ $CeNi_2Ge_2$	C. Frost (ISIS)	structure refinement, magnetic structure
$Be(OD)_2$ $Zn(OD)_2$	R. Stahl (Chemistry, U Dortmund)	hydrogen positions
$D_7I_3O_{14}$ $H_7I_3O_{14}$	T. Kraft (Chemistry, U Bonn)	deuterium localisation
DPN_2	R. Nymwegen (Chemistry, U Dortmund)	structure determination
Fe_2N, Fe_3N $Fe_3N_{1.25}$	D. Rechenbach, A. Leineweber (Chemistry, U Dortmund)	structure refinement, magnetic structure

substance	applicant	topic
$HoCo_2$	H. Tietze-Jaensch (ISIS, U Bonn)	magnetic spin fluctuations
KDS	F. Haarmann (Chemistry, U Dortmund)	orientational disorder
KND_2	M. Müller (Physics, U Kiel)	orientational disorder
$KTaN_2$	H. Stegen (Chemistry, U Dortmund)	nitrogen localization
$LaFe_{10.8}Al_{2.2}N_{2.5}$ $LaFe_{10.9}Al_{2.1}$	O. Moze (Physics, U Parma)	magnetic structure
$Li_2X(OD)$, X=Cl,Br $LiBrD_2O$	C. Eilbracht (Chemistry, U Dortmund)	orientational disorder
$NaND_2$	J. Senker (Chemistry, U Dortmund)	orientational disorder
$NaFeGe_2O_6$	M Behruzi (Cystallogr., TH Aachen)	magnetic structure
$Na_2[Sn(ND_2)]_6$	F. Flacke (Chemistry, U Dortmund)	deuterium localization
$3PbBr_2\ 2D_2O$	Prof Keller (Chemistry, U Dortmund)	deuterium localization
$RbLi_2(ND_2)_3$ $RbLi(ND_2)_2$	P. Bohger (Chemistry, U Dortmund)	orientational disorder
Rb_2MnCl_4	H. Tietze-Jaensch (ISIS, U Bonn)	magnetic phase diagram
$Re_4H_4CO_{12} + C_6H_6$	N. Masciocci (Chemistry, U Mailand)	hydrogen positions
Sr_2ND	T. Sichla (Chemistry, U Dortmund)	deuterium localization
$Sr(OD,H)_2$	S. Peter (Chemistry, U Siegen)	deuterium localization
$Tb_2Co_{10}Ga_7$ $Tb_2Co_{16}Ga$	O. Moze (Physics, U Parma)	site occupation, magnetic structure
$TbCo_{1-x}Ni_xC_2$ (x=0.15,0.3,0.5,0.7,0.85)	J. Yakinthos, W. Kockelmann (Physics, U Xanthi; U Bonn)	magnetic structure
$Y(Co,Mn)_2Si_2$	M. Hofmann (ISIS)	magnetic structure
$Zn_{0.5}Li_{0.5}Ti_{1.5}O_4$	E. Rönsch (Chemistry, TU Dresden)	cation distribution
ZnO	W. Potzel (Physics, TU München)	thermal expansion anomaly
Zn_2SiO_4	E. Rönsch (Chemistry, TU Dresden)	atom positions

3. Usage of the Instrument

In fact, ROTAX was born with the spirit of developing new methods, technique and technology. Despite the fact that the inelastic option for highly advanced crystal analyser spectroscopy is not to be followed any longer, ROTAX still provides an ideal test bed for developing other innovative methods of neutron scattering. Nevertheless, the day-to-day bread winning business is be high quality tof-diffraction (see chapter 3.1). However, there always needs to be the motivation for novel developments. Some examples of new applications of ROTAX are briefly mentioned in chapter 3.2.

3.1 Operation of ROTAX

The conversion of ROTAX from a spectrometer to a diffractometer was straightforward and accomplished without any principal problems. However, its beam-line position behind PRISMA is not ideal because of the neutron flux reduction due to the PRISMA sample. On the other hand, the PRISMA instrument, especially the background chopper, provides good shielding against background-producing fast neutrons. No improvement to the beam-line itself and to the in-pile beam optics has been made yet, nor has the openly built secondary part of the machine been much altered. Measures to improve instrument background are decribed in chapter 3.1.2.

Most of the control software had to be changed or modified since the data analysis software for diffraction is completly different to what was needed for ROTAX as a spectrometer. Therefore, we applied ourselves to install links and file converters to utilise existing software packages available at ISIS and KFA Jülich. This is a continuing process, however, even early results from ROTAX experiments were of high quality and to their users satisfaction. Routine analysis of powder diffraction diagrams is performed using the ISIS software package, which is based on the Cambridge crystallographic subroutine library (CCSL) or other time-of-flight analysis programs like GSAS.

ROTAX is served by the ISIS sample environment pool, i.e. all existing ISIS cryostates, furnaces, magnets etc. are available for use on ROTAX.

3.1.1 Example of a powder diffraction measurement

As an example of a diffraction measurement on ROTAX Fig. 3.1 shows the data collected from iron nitrite Fe_3N (A. Leineweber, H. Jacobs, U Dortmund). Data were collected in the standard setup with one detector in forward scattering (25 - 65 °, Figs. 3.1 a, c, e) and one detector unit in the backscattering regime (105 - 145 °, Figs. 3.1 b, d, f). The two detectors cover a range of d-spacings from 0.3 - 8 Å. The two dimensional raw data files (Figs. 3.1 a, b) were normalized to the incoming neutron flux distribution (Figs. 3.1 c, d) and then converted to a one dimensional d-value pattern (Figs. 3.1 e, f).

***Tab. 3.1:** refined parameters of Fe_3N at T=4 K*

space group:	$P6_322$		
lattice parameters:	a = 4.6856(1) Å c = 4.3608(1) Å		
	x/a	B_{iso}	$\mu_\perp$
Fe 6(g)	0.3263(2)	0.16(2) Å^2	2.23(2) μ_B
N 2(c)	-	0.28(3) Å^2	-
R_{wp} = 4.2 % R_{Bragg} = 5 %			

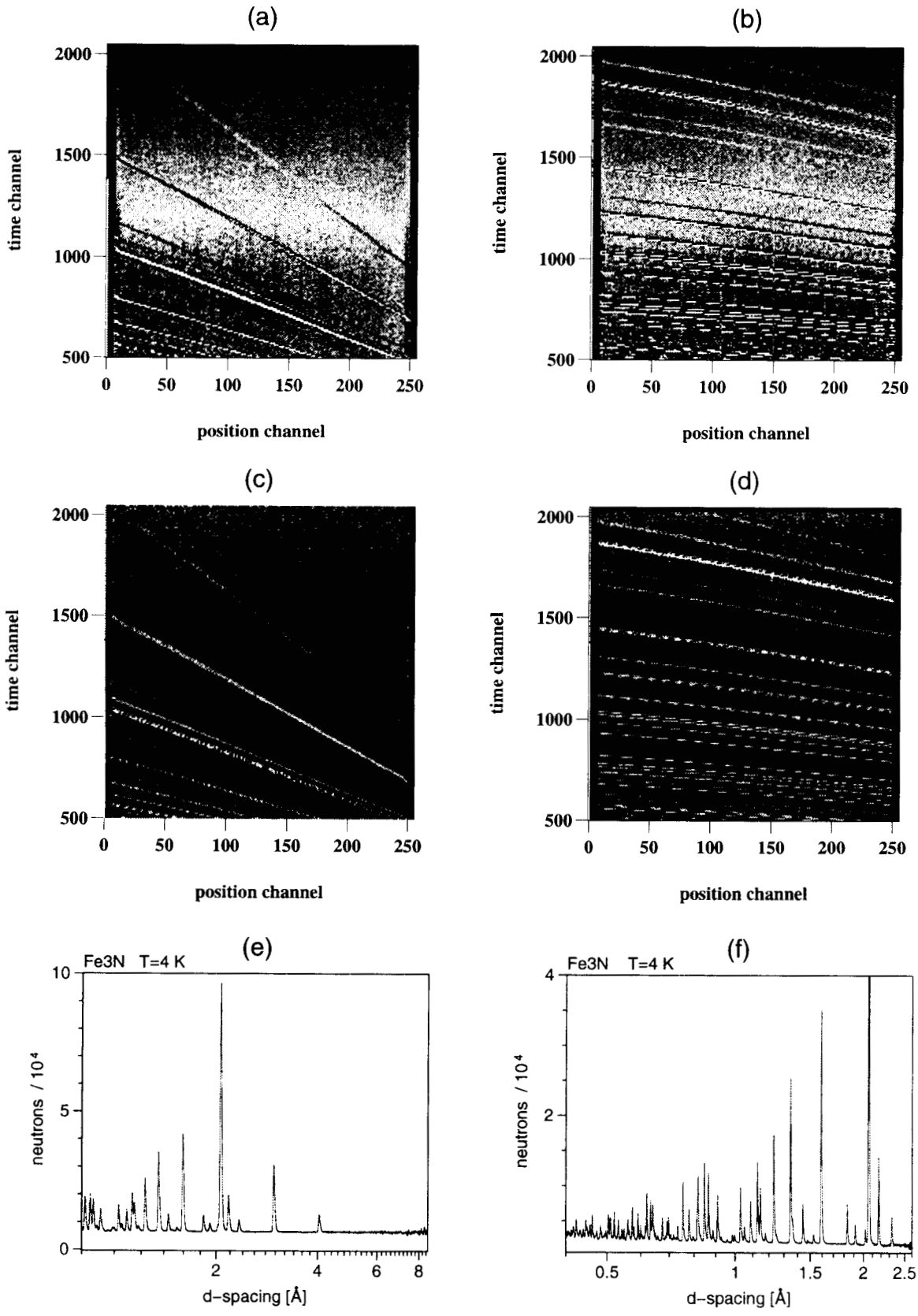

Fig. 3.1: *A measurement on ROTAX: example of Fe_3N. (a),(b) unnormalised raw data intensities vs. time-of-flight and position channel for detectors at 2Θ=45.1° and 124.5°. (c), (d) the corresponding normalised intensity patterns and (e), f) diffraction patterns of Fe_3N from JULIOS 1 and JULIOS 2, respectively, after d-spacing histogramming (focussing). These files are ready for further refinement*

The data were analysed with the GSAS program package [6]. Fig. 3.2 shows observed and refined calculated profiles. The refinement parameters are summarized in Tab. 3.1. The analysis of the data revealed the existence of a ferromagnetic order of the iron moments $\mu_\perp$ perpendicular to the c-axis. Disentanglement of the magnetic and thermal parameters was achieved only by taking advantage of the wide d-value range available.

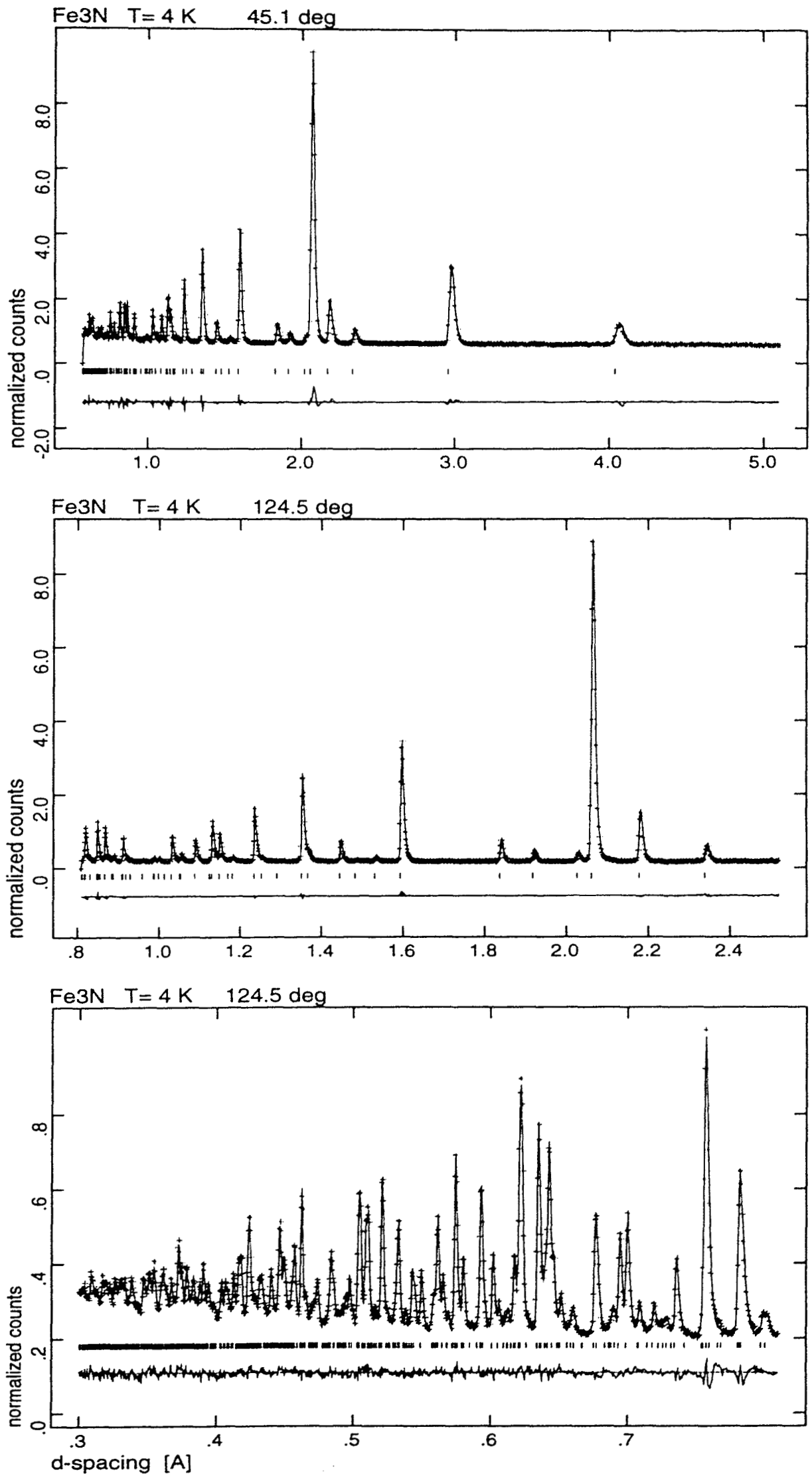

Fig. 3.2: *Refined diffraction patterns of Fe_3N. Top: low angle (45.1°) pattern from Julios 1; centre: high angle pattern from Julios 2 at 0.9 - 5 Å d-spacings; bottom: high angle pattern from Julios 2 at 0.3 - 0.9 Å d-spacings.*

3.1.2 Technical Improvements

Background reduction:

The most severe limitation on ROTAX arises from a high instrument background. Unlike the spectrometer application of ROTAX, there is no use of Soller collimators for the diffractometer because the scattered flight path is deliberately being kept wide open. Both Julios detector units need to be operated with variable centre positioning in order to accommodate all requests from specific crystal alignment set-up to wide range powder diffraction and novel tof-texture measurements. The installation of an evacuated sample tank has reduced instrument background on ROTAX already significantly, especially for measurements at ambient temperatures.

We do believe that there is still some room for further improvements: a divergent secondary flight path collimator will vastly reduce off-centre scattering from vacuum or cryostat windows. Thanks to the tof-diffraction technique it will not require any oscillation. At present such a device is under construction and we will need some experience about how densely packed and at what angle and optimum distance the divergent collimator blades, made of 0.3 mm thick B_4C coated glass, must be placed.

New data file formats:

A new compact binary file format was introduced. This became necessary because of

i) a second Julios detector,

ii) new timer card with much increased time range and time resolution,

iii) inclusion of the monitor spectrum into the data file for on-line normalisation,

iv) revised file-header which now includes all information about the setting of the instrument, control and sample environment parameters.

This new file format is incompatible with the old one, i.e. old programs had to be revised too. However, a format type label enables the new software to automatically recognise and read old formatted files.

Remote and command file control of the temperature is now installed. The synchronisation of both JULIOS detector units is performed via mailboxes on a common network directory.

Analyser drive:

The ROTAX analyser drive was kept operational although it was not used for any experiment. However, an improvement of tremendeous importance has been achieved: The introduction of specifically designed choking coils between inverter (main amplifier) and analyser motor. The function of the coils is to attenuate all unneccessary high-frequency noise on the 30 m long power cable. As a result the ROTAX analyser now runs reliably and to its design specifications. The problem of the limited life-time of the analyser motor due to the long power cable and its high capacitance has been solved. A long term test run for more than 6 weeks without disruption has been completed without any fault condition on the ROTAX drive. Thus, the ROTAX drive is available not only for neutron spectroscopy but also for single crystal double diffraction (for which there is sufficient flux) and real-time experiments, another useful application of the analyser drive.

Magnetic shield for JULIOS detector:

The use of the ISIS cryo-magnet (7.5 T vertical) exposes the phototubes of the Julios detector to a stray field of 150 Gauss, too much for a safe operation of the detector. Shields made of a soft-iron / μ-metal sandwich are placed all around the detector. The internal magnetic shield of a straight μ-metal box proved insufficient, because its surface is perpendicular to the field lines. The trick with the new shield is that 1.) it traps the magnetic stray field lines at an angle and 2.) it releases them again at the bottom in order to close the field loop. This ROTAX-type shield is being copied by other ISIS instruments and it prevents a lengthy "degaussing programme" after the use of the ISIS cryo-magnet.

ISIS DAE link:

A hardware-link from the Julios electronics to the standard ISIS detector electronics has been installed for both detector units. This allows use of our detector set-up for data aquisition and instrument control via CAMAC and VAX computers. With this link a long outstanding request by the ISIS managment was fulfilled to use ROTAX like all the other ISIS instruments. Users of the ALF facility (ISIS crystal aligment facility) make frequent use of this JULIOS to ISIS-DAE link.

3.1.3 Computer structure

There is a set of networked computers for the control of the instrument, the data acquisition and analysis. For each JULIOS detector a Pentium PC is installed for the control of the particular experiment: they are being used for set-up and calibration of the detectors as well as performing command files for highly automised measurements. They talk to external temperature controllers and the remote control computer for the compressed air pads and stepper motors via RS232 serial interfaces. The MicroVAX serves the local subnetwork where the datasets are eventually transferred to. Common network directories hold mailboxes for the synchronisation of the two detectors. Either a DecNet or a TCP/IP protocol can be run. The Vax serves as a communication node to subsequent ISIS computers and electronics. A replacement with a more up to date Alpha-VMS station is pending where we aim to bundle VMS based data analysis and user software.

ROTAX diffraction data files can be treated with GSAS or transported into GENIE, the ISIS standard general data visualisation software. Either directly or using the GENIE platform, ROTAX files can also be treated with programs using the CCSL libraries.

For single crystal and inelastic data treatment the use of Spyglass Transform and Origin software is available in addition to self-written packages specifically designed for the ROTAX analyser option. The latter, however, have not been updated or further developed for the past two years.

The ROTAX MicroVAX / Alpha station is included into the ISIS campus network and internetted for direct FTP and WEB access. Help files, instrument reports and user manuals are available on-line.

3.1.4 New Acquisitions

There were four major purchases to complement and upgrade the ROTAX instrument:

Second JULIOS detector unit:
A second linear position sensitive JULIOS detector unit was acquired in early 1995. It is placed on a temporary mechanical set-up at a fixed backscattering position at a centre angle of ϕ_{02}=124.5 ° at a secondary flight path length of 1.134 m and covers $\Delta\Theta$≈40 ° of scattering angle or a range of d-spacing values between 0.3 and 3 Å.

Orange-type cryo-furnace:
Our initial contribution to the ISIS sample environment pool was the purchase of a cryo-furnace for 2 - 600 K temperature range and ±0.1° stability. Equipped with a 360° window and vanadium tails this device is particularly dedicated for diffraction. ROTAX has first priority on this kit, however any other equipment from the pool can used in exchange after prior arrangement.

Alpha-station for Micro-Vax replacement:
After ten years troublefree operation our MicroVAX front-end computer has been replaced with a more up-to-date and powerful Alpha-500 (VMS) station.

Sample vacuum vessel and pump system:
Our efforts to reduce the instrument background level required the purchase of a sample vacuum vessel and an attached pump system. In order to minimize the costs we made use of the old POLARIS tank. Despite not having its windows in an optimum position, a vast background reduction was achieved. A divergent scattered flight path collimator is under construction. Its collimator blades were provided free from LNPS Gatchina, Russia.

3.2 Novel Applications of the Instrument

3.2.1 ROTAX Texture Diffractometer Option

The potential use of ROTAX as a texture diffractometer has been investigated. Texture represents the orientational distribution of crystallites in a polycrystal. Three dimensional orientation distribution functions are obtained from two-dimensional pole-figures of Bragg reflections hkl which are obtained by scanning the sample through the whole range of different sample orientations. Taking advantage of the pulsed white neutron beam at ISIS together with a position sensitive detector, the number of different sample settings is only a small fraction of what would be required in constant-λ pole figure measurements at a reactor source. This is primarily due to the fact that the conventional pole distance χ is automatically included in the time-of-flight technique [4,5, 7,8].

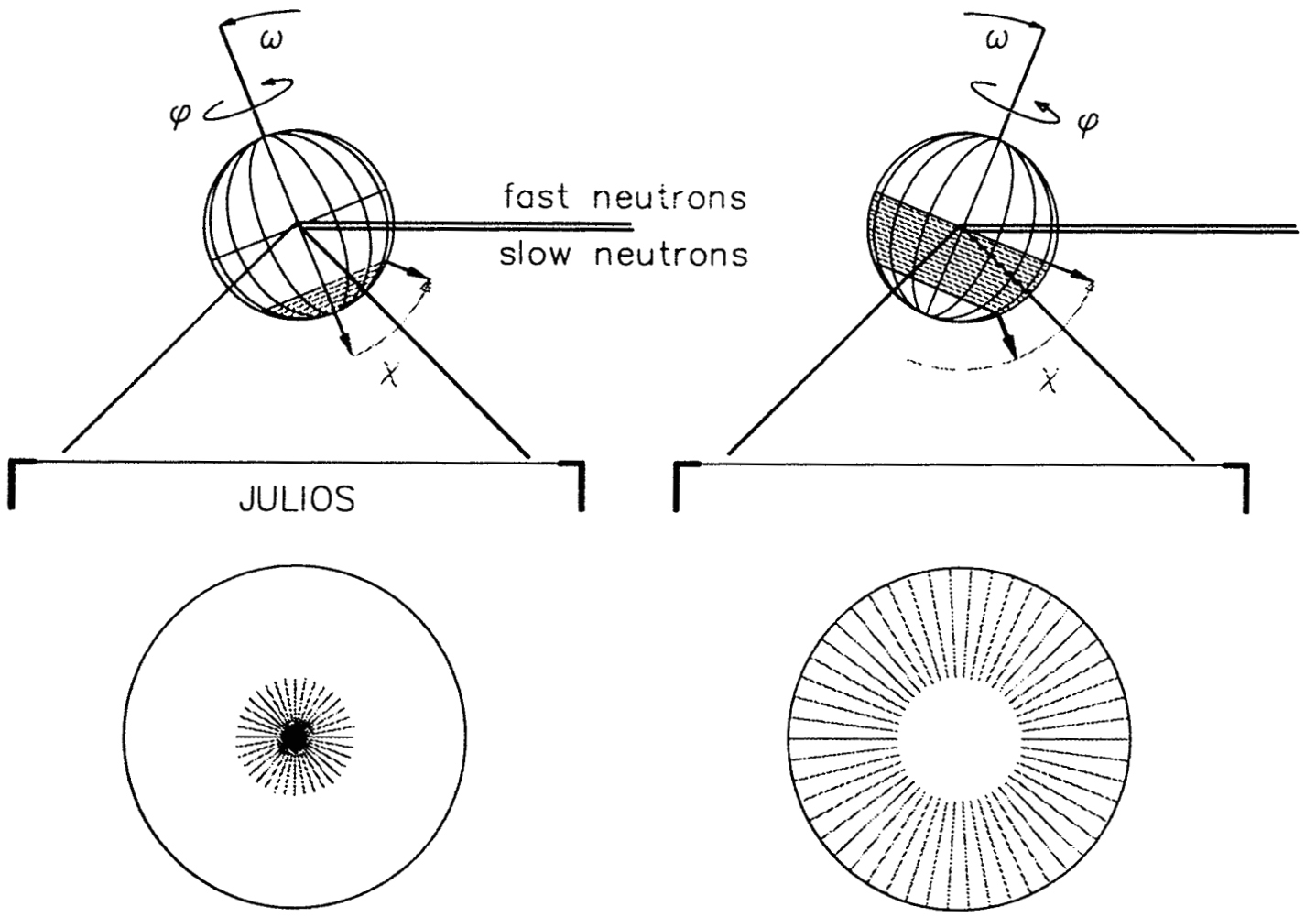

Fig. 3.3: *Reference pole sphere settings and scanning patterns for a TOF texture diffractometer*

Fig 3.3 illustrates how one hemisphere of the reference pole sphere around the sample is covered using a position sensitive detector, an ω-turntable and a φ-one-circle goniometer. Just two ω-positions are required if the detector covers $\Delta 2\theta=90°$, corresponding to $\Delta\chi=45°$. Test measurements have been performed on ROTAX using one JULIOS detector at $2\theta=90°$ and covering a range $\Delta 2\theta=33°$ (see Fig. 3.4). In this case three ω settings, each scanning a complete azimuthal circle of 360°, were required to scan the whole hemisphere.

Pole figures of various samples (see Tab. 3.2) of known texture were measured. The scan grid used comprised 120 orientations for each sample. With counting times of 2-5 minutes per Δφ-step the data collection time for a complete grid of each sample was 4-10 hours, i.e. 5-10 times faster than the same measurements performed in Jülich for comparison. As an example, Fig 3.5 shows 6 measured pole figures of a copper sample which were measured simultaneously by taking advantage of the white beam tof-technique.

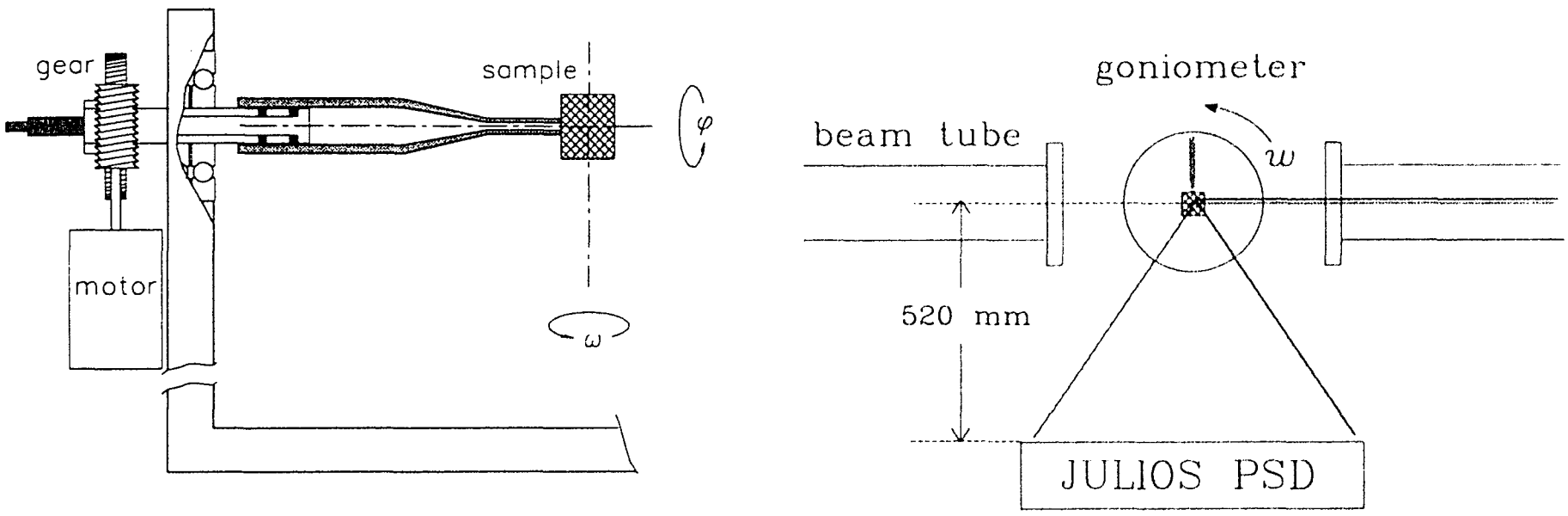

Fig. 3.4: One-circle goniometer and experimental setup

Tab. 3.2: Samples measured on ROTAX for tests purposes

specimen:	sample from	scan grid
cold-rolled Co	J. Palacios, Univ Mexico City	ω = -30°, Δφ = 7.2°
ZnAl	J. Palacios, Univ Mexico City	ω = 0°, Δφ = 8.0°
Mylonite	H. Kern, Univ Kiel	ω = +30°, Δφ = 14.4°
Quarzite	H.R. Wenk, Univ Berkeley	in total: 120 individual
Haematite	H. Siemes, Univ Aachen	orientation settings

The data collection times can be reduced further by using a minimum of two ω-settings with the detector closer to the sample. This will reduce the number of necessary scan points and increase the scattered intensity, but will compromise the resolution of the Bragg reflections, not a problem where lines are well separated.

The rapid collection of complete pole figures also allows to economically reverse the method: the texture diffractometer setup can be used to measure, within reasonable times, the d-value spectrum of a polycrystalline sample, integrated over all possible orientations which otherwise would have suffered from (multiple) preferred orientation of the crystallites. Then the resulting spectrum, integrated over all sample orientations, can be used for "texture-free" analysis. Furthermore, the diffraction intensities obtained from

one individual sample orientation can be related to the orientation-integrated and averaged intensities by generating a reference table. This table can be utilised to investigate a texturized sample at different temperatures e.g. in a cryostat which only allows the setting of one sample orientation conveniently.

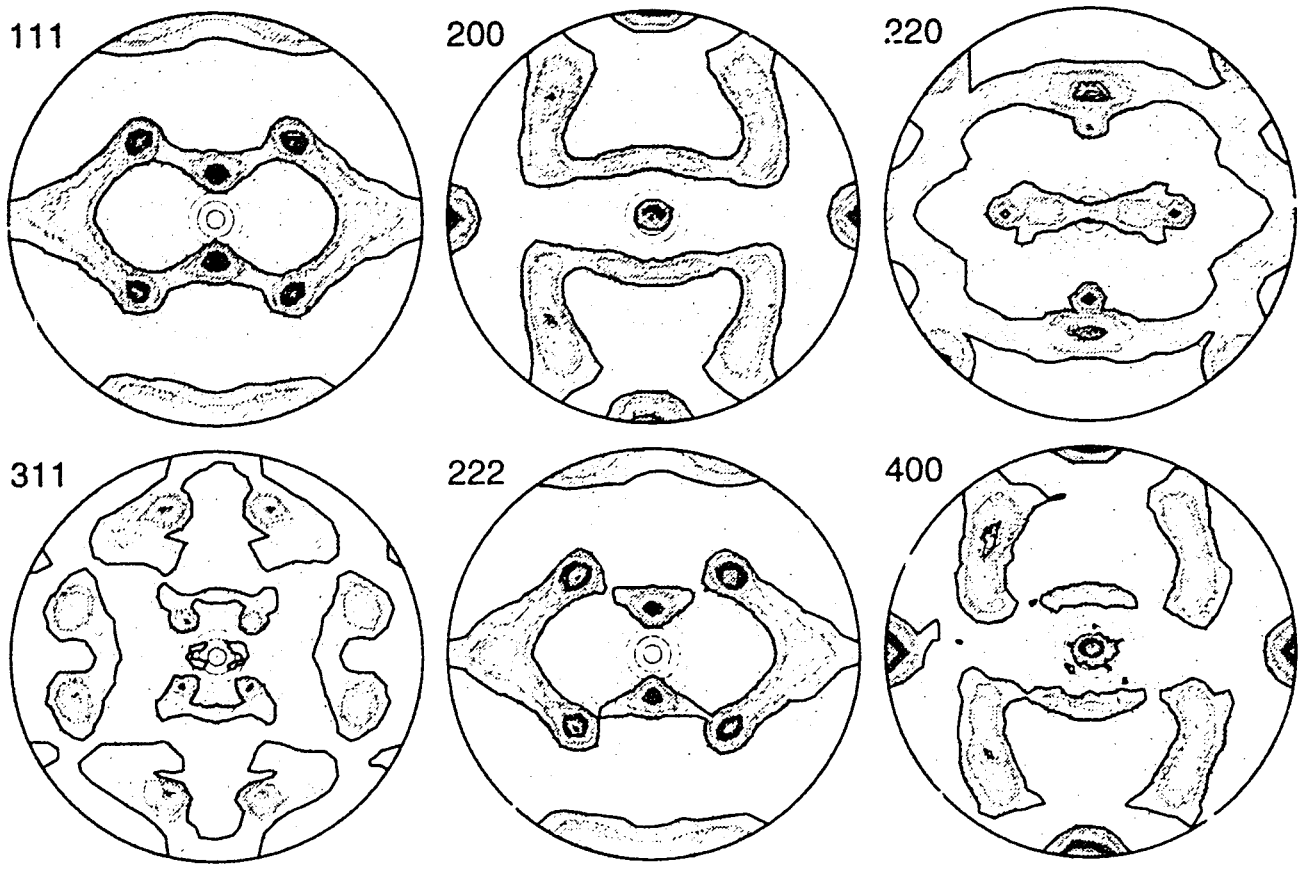

Fig. 3.5 Experimental pole figures of rolled copper

3.2.2 ROTAX/DIFF for wide Q-range diffuse scattering

Diffraction on ROTAX provides a large range of Q- or d-values extending over more than one order of magnitude. The 2-dimensional data imaging (intensities vs. tof and 2Θ) in combination with the excellent contrast properties of the JULIOS detector ROTAX provides a promising possibility for wide Q-range diffuse scattering. Test and demonstration experiments are under preparation.

3.3 Staff News

In early 1995 Dr. W. Kockelmann joined the ROTAX team. His scientific background is in crystallography and powder diffraction. On 1 April 1995 Prof. G. Will (University of Bonn) took over the project-leadership from Prof. G. Landwehr (University of Würzburg) who was in charge temporarily for one year after Prof. R. Geick's (the ROTAX initiator) retirement. The responsibility for the ROTAX instrument was transferred from the Physics Institute of the University of Würzburg to the Mineralogical Institute of the University of Bonn. At the end of July 1995 Dr. W. Schmidt left the ROTAX team and took up a new position at the ILL. We wish to thank him for his highly committed work on ROTAX, he played a very important role in technically developing and devising the novel rotating analyser drive. On 1 October 1996 Prof. A. Kirfel succeeded Prof. G. Will at the Institute of Mineralogy and Petrology in Bonn and, thus, became new head of the ROTAX project. At the end of this transition period Dr. H. Tietze-Jaensch is the only member of the ROTAX team who had worked for it continuously from its very beginning.

3.4 Collaboration with ISIS

On 1 April 1995 when the University of Bonn officially took over the ROTAX project our UK partner reorganised, too. The Council of the Central Laboratory of Research Councils (CCLRC) came into existence. A renewal of the former collaboration agreement was exchanged between CCLRC and Bonn University, after both partners found the collaboration between SERC and the University of Würzburg had worked to mutual satisfaction.

4. Beam Usage and Statistics

The available beam time on ROTAX was shared in equal parts between all ISIS users and German scientists (Fig. 4.1). Instrument time used for installation of new components, calibration and off-time caused by any faulty condition of an integral part of the instrument is counted separately. There has been some lost beam time caused by extra closures of the whole beam line due to installation work on the upstream instrument PRISMA or because of special experiments on PRISMA, counted against the UK fraction on ROTAX. On, average ROTAX has achieved 89 % actual beam usage for scientific experiments and technical developments (see Tab. 4.1 for details).

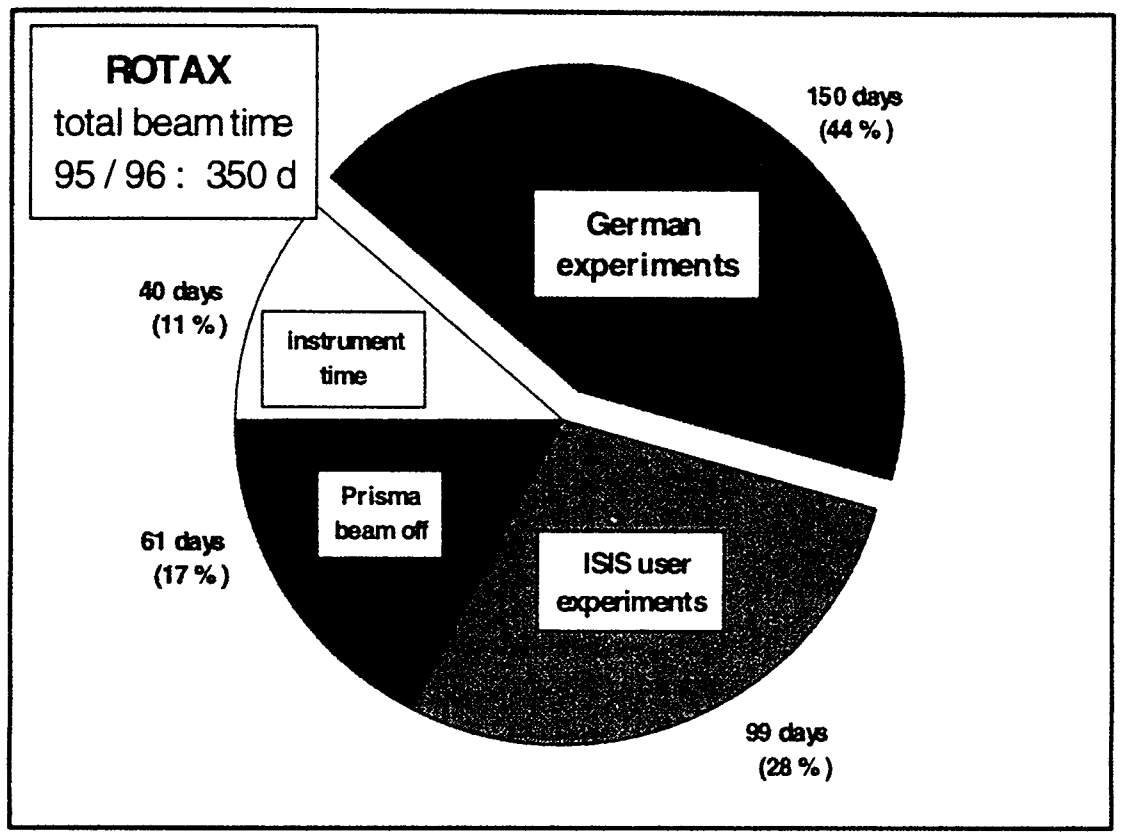

Fig. 4.1: Country shares and fractions of beam time usage on ROTAX in 1995 - 1996

Tab. 4.1: ROTAX beam usage and performance statistics

cycle		available beam time (days)	ROTAX days of usage	beam usage by instrument	instrument off, installation, calibration	number of experiments

	month	year	ISIS	beam to ROTAX	UK days	D days	days	%	days	%	
94/5	1-2	1995	35	35	24	8	32	91	3	9	5
94/6	2-3	1995	31	31	19.5	9.5	29	94	2	6	12
95/1	5-6	1995	31	0	0	0	0	0	0	0	0
95/2	6-7	1995	24	11.5	0	9	9	78	2.5	22	9
95/3	8-9	1995	32	32	7.5	19.5	27	84	5	16	4
95/4	10	1995	31	31	4.5	18.5	23	74	8	26	11
95/5	11-12	1995	36	26	3.5	18	21.5	83	4.5	17	16
95/6	1	1996	22	22	2	16	18	82	4	18	9
96/1	6-7	1996	45	42	4.5	32	36.5	87	5.5	13	20
96/2	9	1996	28	28	20	6	26	93	2	7	18
96/3	11-12	1996	35	29	13	13	26	90	3	10	17
summary		**1995/96**	**350**	**287.5**	**98.5**	**149.5**	**248**	**86**	**39.5**	**14**	**121**

5. Beam Time Applications

For the German fraction beam time application is simple and informal. Applicants may contact the project leader or one of the instrument scientists at RAL at any time (Tab 4.2), i.e. there are no deadlines. We then kindly request the user to submit a ROTAX application proposal. The scientific aim and technical feasibility will be discussed in due course. Successful applications will be granted beam time, usually within 6 months. On ROTAX we do not stick exactly to the requested experiment days, rather we adopt the policy that an experiment or project should be finished to the user's satisfaction and that he or she should return home with data sets worthwhile for on-going analysis. Thus, we cannot precisely calculate oversubscription factors for ROTAX.

There is also the possibility to apply for ROTAX through the standard ISIS beam time application procedure for the ISIS fraction on ROTAX. For details, please contact the ISIS web page (http://www.isis.rl.ac.uk) or phone the university liaison office at RAL (++44-1235-44.5592) or contact the instrument scientists. Deadlines for receipt of applications are twice yearly on April 16th and October 16th.

The instrument operates within the Excitation Group (Leader Dr. U. Steigenberger) in the ISIS Spectroscopy Support Division (Head Dr. C. J. Carlile).

Tab 4.2: *Contact the ROTAX team*

name	***address***	***phone***	***fax***	***e-mail***
Prof. Dr. Armin Kirfel	Mineralogisches Institut, University of Bonn Poppelsdorfer Schloss D-53115 BONN Germany	++49-228-73.2761	++49-228-73.2770	A.Kirfel@uni-bonn.de
Dr. Holger Tietze-Jaensch	Rutherford Appleton Lab. ISIS Facility R3 ROTAX Chilton, Didcot OX11 0QX United Kingdom	++44-1235-44.5685	++44-1235-44.5720	H.Tietze@rl.ac.uk
Dr. Winfried Kockelmann	Rutherford Appleton Lab. ISIS Facility R3 ROTAX Chilton, Didcot OX11 0QX United Kingdom	++44-1235-44.6731	++44-1235-44.5720	W.Kockelmann@rl.ac.uk

6. References

[1] A. D. Taylor
RAL report, RAL-84-120 (1984).

[2] W. I. F. David, D.E. Akporiaye, R.M. Ibberson and C.C.Wilson
HRPD User Guide (1988).

[3] W.I.F. David and J.D. Jorgensen
IUCr Monogr. Crystallogr, Vol 5, (ed. R.A.Young).
Oxford University Press, Oxford 1993, pp 197.

[4] W. Schäfer, E. Jansen, W. Kockelmann, H. Tietze-Jaensch and G. Will
Setup and operation mode of a pulsed white beam angle dispersive TOF-texture diffractometer
ICANS XIII, PSI Proceedings 95-02 I-6 (1995) 87

[5] W. Schäfer, E. Jansen, R. Skowronek, G. Will, W. Kockelmann, W. Schmidt and
H. Tietze-Jaensch
Setup and use of ROTAX as an angle-dispersive neutron powder and texture diffractometer
Nucl. Instrum. Methods A 364 (1995) 179

[6] A.C. Larson and R.B. von Dreele
GSAS User Manual, LANL report LAUR 86-748 (1986).

[7] K. Feldmann
Experimental Techniques of Texture analysis, 1986 (ed. H.J. Bunge).
DGM Informationsgesellschaft Verlag Oberursel, pp. 253-263.

[8] E. Jansen, W. Schäfer, W. Kockelmann and G. Will
Multiple pole figure extraction from pulsed white beam angle dispersive neutron diffraction data.
Textures and Microstructures 26-27 (1996) 11.

Appendix:

A1: Comprehensive List of Publications about ROTAX

1.) R. Geick, H. Tietze
Proposal for a rotating analyser single crystal spectrometer at a pulsed neutron source
Nucl. Instr. Meth. A249 (1986) 325

2.) H. Tietze, R. Geick
The rotating analyser crystal spectrometer ROTAX
Proc. Int. Collab. Advanced Neutron Sources ICANS IX 1986, CH-Villigen,
Switzerland, SIN-rep. 40926 (1987) 389

3.) W. Schmidt, H. Tietze, R. Geick
Technical feasibility of the ROTAX analyser drive and its influence on the
performance of the spectrometer
Proc. Int. Conf. on Neutron Scattering ICNS'88, Grenoble (1988)
Physica B 156 (1989) 554

4.) H. Tietze, W. Schmidt, R. Geick
ROTAX, a spectrometer for coherent neutron inelastic scattering at ISIS
Proc. Int. Conf. on Neutron Scattering ICNS'88, Grenoble (1988)
Physica B 156 (1989) 550

5.) H. Tietze, W. Schmidt, R. Geick, H. Samulowitz, U. Steigenberger
Set-up and optimization of scans with the rotating analyser crystal spectrometer ROTAX
Proc. Neutron scattering data analysis conf. WONSDA II, Rutherford (1990),
IOP Conf. Series 107 (1990) 253

6.) H. Tietze, W. Schmidt, R. Geick, U. Steigenberger, H. Samulowitz
Neutron scattering on ROTAX
Proc. Int. Collaboration on Advanced Neutron Sources ICANS XI 1990,
KEK Japan, KEK report 90-25 (1991) 774

7.) H. Tietze-Jaensch, W. Schmidt, D. Sieger, R. Geick, U. Steigenberger
Neutron scattering on ROTAX
Proc. Int. Conf. on Neutron Scattering ICNS'91, Oxford (1991),
Physica B 180 & 181 (1992) 920

8.) E. Jansen, W. Schäfer, A. Szepesvary, R. Reinartz, H. Tietze, G. Will, K.D. Müller,
U. Steigenberger
PSD JULIOS under experimental conditions at ISIS
Proc. Int. Conf. on Neutron Scattering ICNS'91, Oxford (1991),
Physica B 180 & 181 (1992) 917

9.) H. Tietze-Jaensch, W. Schmidt, R. Geick
Performance of ROTAX
Proc. Int. Collaboration on Advanced Neutron Sources ICANS XII 1993,
Abingdon U.K.1993, RAL rep. 94-025, p. 97-I

10.) W. Schmidt, H. Tietze-Jaensch, R. Geick
New Scans and Data Visualisation on ROTAX
Proc. Int. Collaboration on Advanced Neutron Sources ICANS XII 1993,
Abingdon U.K.1993, RAL rep. 94-025, p. 292-I

11.) H. Tietze-Jaensch, W. Schmidt, R. Geick
ROTAX, a neutron time-of-flight spectrometer with a non-uniformly spinning analyser
Int. Conf. Neutron Scattering, Sendai Japan, 1994
Physica B 213&214 (1995) 878-880

12.)W. Schmidt, H. Tietze-Jaensch, R. Geick
Scan preparation and data interpretation on ROTAX
Int. Conf. Neutron Scattering, Sendai Japan, 1994
Physica B 213&214 (1995) 881-883

13.) H. Tietze-Jaensch. W. Schmidt, R. Geick, G. Will
Evaluation of ROTAX
ICANS XIII, PSI Proceedings 95-02 I-6 (1995) 130

14.)W. Schäfer, E. Jansen, W. Kockelmann, H. Tietze-Jaensch, G. Will
Setup and operation mode of a pulsed white beam angle dispersive TOF-texture diffractometer
ICANS XIII, PSI Proceedings 95-02 I-6 (1995) 87

15.) W. Schäfer, E. Jansen, R. Skowronek, G. Will, W. Kockelmann, W. Schmidt, H. Tietze-Jaensch
Setup and use of the ROTAX instrument at ISIS as angle-dispersive neutron powder and texture diffractometer
Nucl. Instrum. Methods A 364 (1995) 179

16.)W. Schäfer, W. Kockelmann, E. Jansen, W. Schmidt, H. Tietze-Jaensch, G. Will
A versatile neutron powder time-of-flight diffractometer of wide d-spacing coverage
Proc. EPDIC-IV, Materials Science Forum 228-231 (1996) 259

17.) E. Jansen, W. Schäfer, W. Kockelmann, G. Will
Multiple pole figure extraction from pulsed white beam angle dispersive neutron diffraction data
Textures and Microstructures 26-27 (1996) 11

18.) H. Tietze-Jaensch, W. Schmidt, R. Geick
Evaluation of the ROTAX Spectrometer
Proc. ECNS'96, Interlaken, 1996, to be publ. in Physica B

19.) H. Tietze-Jaensch, W. Kockelmann, W. Schmidt, G. Will
The ROTAX / DIFF Time-of-Flight Diffractometer at ISIS
Proc. ECNS'96, Interlaken, 1996, to be publ. in Physica B

20.) H. Tietze-Jaensch
Evaluation and optimised design of a ROTAX type instrument
Workshop on instrument design, LBL Berkeley 1996, to be published

A2: Other Publications with ROTAX involved

1.) W. Schiessl, W. Potzel, H. Karzel, M. Steiner, G.M. Kalvius, A. Martin, M.K. Krause, I. Halevy, J. Gal, W. Schäfer, G. Will, M. Hillberg, R. Wäppling
Magnetic properties of the $ZnFe_2O_4$ spinel.
Phys. Rev B53 (1996) 9143

2.) W. Potzel, M. Kalvius, W. Schiessl, H. Karzel, M. Steiner, A. Kratzer, A. Martin, M.K. Krause, A. Schneider, I. Halevy and J. Gal, W. Schäfer, G. Will, M. Hillberg, R. Wäppling, D.W.Mitchel and T.P. Das
Dynamic short-range order observed in the $(Zn)[Fe_2]O_4$ spinel by neutron diffraction, mSR and Mössbauer experiments.
Hyp. Int. 97 (1996) 373

3.) M. Müller, B. Asmussen, W. Press, J. Senker, H. Jacobs, H. Büttner, W. Kockelmann, R.M. Ibberson
Dynamics of the amide ions in potassium amide: orientational order and disorder
Proc. ECNS'96, Interlaken, 1996, to be publ. in Physica B

4.) C. Eilbracht, H. Jacobs, W. Kockelmann, D. Hohlwein
Orientational disorder in perovskite like structures Li2X(OD) (X=Cl,BR) and LiBr*D2O
Proc. ECNS'96, Interlaken, 1996, to be publ. in Physica B

5.) F. Flacke, W. Kockelmann, D. Hohlwein, H. Jacobs
Hydrogen atom orientation in alkali metal hexaamidostannates(VI) $M_2(Sn(NH_2)_6$ (M = Na, K, Rb, Cs)/$M_2(Sn(ND_2)_6$.
Proc. ECNS'96, Interlaken, 1996, to be publ. in Physica B

6.) M. Müller
Anordnung und Dynamik der NH_2-Ionen in Kalium- und Strontiumamid: Untersuchungen mit Neutronenstreuung
Dissertation Universität Kiel (1996)

7.) M. Müller, J. Senker, B. Asmussen, W. Press, H. Jacobs, W. Kockelmann, H.M. Mayer, R.M. Ibberson
Orientational order and rotational dynamics of the amide ions in potassium amide. I. Neutron diffraction
submitted to J. Chem Phys

A3: Publications of the ROTAX team in 1995 / 1996

1.) **H. Tietze-Jaensch**, W. Schmidt, R. Geick
ROTAX, a neutron time-of-flight spectrometer with a non-uniformly spinning analyser
Physica B 213&214 (1995) 878

2.) W. Schmidt, **H. Tietze-Jaensch**, R. Geick
Scan preparation and data interpretation on ROTAX
Physica B 213&214 (1995) 881

3.) W. Schmidt, C. Brotzeller, P. Schweiss, **H. Tietze-Jaensch**, R. Geick, W. Treutmann
Magnetic excitations in Co2SiO4
J. Magn. Magn. Mater. 140-144 (1995) 1989

4.) W. Schmidt, **H. Tietze-Jaensch**, R. Geick, G. Will, H. Grimm
Improvements in resolution calculation for Triple axis and time-of-flight
Proc. Int. Collaboration on Advanced Neutron Sources ICANS XIII 1995, PSI Villigen, ICANS XIII, PSI-Proceedings 95-02 I-13 (1995) 184

5.) **H. Tietze-Jaensch**. W. Schmidt, R. Geick, G. Will
Evaluation of ROTAX
ICANS XIII, PSI Proceedings 95-02 I-6 (1995) 130

6.) W. Schäfer, E. Jansen, **W. Kockelmann, H. Tietze-Jaensch**, G. Will
Setup and operation mode of a pulsed white beam angle dispersive TOF-texture diffractometer
ICANS XIII, PSI Proceedings 95-02 I-6 (1995) 87

7.) W. Schäfer, E. Jansen, R. Skowronek, G. Will, **W. Kockelmann**, W. Schmidt, and **H. Tietze-Jaensch**
Setup and use of the ROTAX instrument at ISIS as angle-dispersive neutron powder and texture diffractometer
Nucl. Instrum. Methods A 364 (1995) 179

8.) W. Schäfer, **W. Kockelmann**, G. Will, P. Fischer, J. Gal
Neutron diffraction on YFe_5Al_7 as reference on the f-magnetism of isostructural rare-earth-iron-aluminium compounds
J. Alloys Compounds 225 (1995) 440

9.) W. Schäfer, **W. Kockelmann**, E. Jansen, W. Schmidt, **H. Tietze-Jaensch**, G. Will
A versatile neutron powder time-of-flight diffractometer of wide d-spacing coverage
Proc. EPDIC-IV, Materials Science Forum 228-231 (1996) 259

10.) E. Jansen, W. Schäfer, **W. Kockelmann**, G. Will
Multiple pole figure extraction from pulsed white beam angle dispersive neutron diffraction data
Textures and Microstructures 26-27 (1996) 11

11.) E. Jansen, W. Schäfer, **W. Kockelmann**, G. Will
Multiple pole figure extraction from pulsed white beam angle dispersive neutron diffraction data
Textures and Microstructures 26-27 (1996) 11

12.) W. Schäfer, **W. Kockelmann**, G. Will, P.A. Kotsanidis, J.K. Yakinthos, W. Reimers
Crystal and magnetic structure of $TbCo_{0.5}Ni_{0.5}C_2$
Z. Krist 211 (1996) 106

13.) B. Bauer, R. Hempelmann, T.J. Udovic, J.J. Rush, **W. Kockelmann**, E. Jansen, W. Schäfer, D.Richter
Structure and microdomain structure of ordered niobium hydrides and deuterides by means of neutron diffraction
J. Alloys Compounds, accepted

14.) W. Schäfer, **W. Kockelmann**, G. Will, J.K. Yakinthos, P.A. Kotsanidis
Magnetic structures of rare earth (R) $RCoC_2$- and $RNiC_2$ compounds
J. Alloys Compounds, in print

15.) W. Schäfer, **W. Kockelmann**, E. Jansen, G Will
Comparative diffraction experiments using monochromatic and pulsed white neutrons
Proc. ECNS'96, Interlaken, 1996, to be publ. in Physica B

16.) **W. Kockelmann**, W. Schäfer, J.K. Yakinthos, P.A. Kotsanidis, G.F.Papathanassiou, J. Linhart
Commensurate and incommensurate magnetic structure components of Tb-(Co,Ni)-dicarbides
Proc. ECNS'96, Interlaken, 1996, to be publ. in Physica B

17.) **H. Tietze-Jaensch**, R. v d Kamp, W. Schmidt, R. Geick, W. Treutmann, P. Vorderwisch
The Magnetic Excitation Spectrum of Rb2MnCl4
Proc. ECNS'96, Interlaken, 1996, to be publ. in Physica B

18.) **H. Tietze-Jaensch**, W. Schmidt, R. Geick
Evaluation of the ROTAX Spectrometer
Proc. ECNS'96, Interlaken, 1996, to be publ. in Physica B

19.) **H. Tietze-Jaensch, W. Kockelmann**, W. Schmidt, G. Will
The ROTAX / DIFF Time-of-Flight Diffractometer at ISIS
Proc. ECNS'96, Interlaken, 1996, to be publ. in Physica B

20.) M. Müller, B. Asmussen, W. Press, J. Senker, H. Jacobs, H. Büttner, **W. Kockelmann**, R.M. Ibberson
Dynamics of the amide ions in potassium amide: orientational order and disorder
Proc. ECNS'96, Interlaken, 1996, to be publ. in Physica B

21.) C. Eilbracht, H. Jacobs, **W. Kockelmann,** D. Hohlwein
Orientational disorder in perovskite like structures Li2X(OD) (X=Cl,BR) and LiBr*D2O
Proc. ECNS'96, Interlaken, 1996, to be publ. in Physica B

22.) F. Flacke, **W. Kockelmann**, D. Hohlwein, H. Jacobs
Hydrogen atom orientation in alkali metal hexaamidostannates(VI) $M_2(Sn(NH_2)_6$ (M = Na, K, Rb, Cs)/$M_2(Sn(ND_2)_6$.
Proc. ECNS'96, Interlaken, 1996, to be publ. in Physica B

A4: Experimental Reports for 1995

This appendix contains the Experimental Reports from experiments carried out on ROTAX in the ISIS cycles 95/1 to 95/6 between May 1995 until February 1996. These report reflect the diffraction activity on ROTAX within the german beam time fraction.

Experimental reports for the ISIS cycles 96/1 to 96/5 are just being requested and will be included in the ISIS 96-97 annual report.

ISIS Experimental Report
Rutherford Appleton Laboratory

RB Number:

Date of Report: march 1996

Title of Experiment: Structure determination of ζ-Fe_2N and ε-$Fe_3N_{1.25}$

Local Contact: W. Kockelmann

Principal Proposer: D. Rechenbach and H. Jacobs

Affiliation: Inorganic Chemistry I, University of Dortmund

Experimental Team: W. Kockelmann, H. Tietze-Jaensch

Instrument: ROTAX / DIFF

Date of Experiment: july/october 1995

Iron nitrides are of fundamental importance for steel production and steel hardening. Up to now details of reactions are unknown e.g. structural information is required in order to obtain reproducible qualities of the hardened steel surface (e.g. [1]). The preparation of single crystals and single phase samples is difficult in account of the low thermal stability and high decomposition pressures of nitrogen at moderate temperatures [2].

Very detailed investigations of binary nitrides of iron were carried out by JACK in the forties and fifties (e.g. [3]-[5]). We found in previous studies [6] that he described the structures in general correctly. In the case of ζ-Fe_2N JACK suggested an orthorhombic distorted hexagonal close packed arrangement of iron atoms with nitrogen atoms in octahedra [3]. He gave no space group and for all atoms in the unit cell twelve atomic positions for an ideal arrangement.

Samples of Fe-powder placed in a corundum container were treated with flowing ammonia in the temperature range of 420 °C to 450 °C and 1 bar total pressure in a glass tube [7]. In agreement with the results obtained by JACK [3] we got single phase products of ζ-Fe_2N.

Guinier diagrams were indexed on the basis of an orthorhombic unit cell. The observed reflection conditions led to the space group Pbcn (No. 60). For a detailed structure analysis neutron powder diffraction data were collected at the Risø National Laboratory (Denmark) with instrument TAS1.

ζ-Fe_2N shows a very small deviation from hexagonal symmetry. The profiles of the reflections in the neutron diffraction diagram are too broad and no splitting was detected. To prove the correctness of the unit cell parameters used so far synchrotron diffraction data were taken at the high resolution powder diffractometer at HASYLAB.

Both sets of data were commonly refined with the program PROFIL [9]. The adaptions of parameters were done in a weighting scheme which depends on the scattering power of the atoms and the information about the different data sets. The wavelength of the synchrotron radiation is very well known. On this basis the wavelength of neutrons was also refined. The final results of technical and crystallographical data are given in Table 1 [6].

In addition we took time-of-flight neutron powder data at the instrument ROTAX (Rutherford, UK). They were refined with the program GSAS [10]. An initial refinement was made starting with the data given above. The main problem was to find a good function for the profile and to handle their parameters during the refinement. A fit between observed and calculated data is illustrated in Figure 1.

A comparison of the results obtained by the two ways mentioned are given in Table 1. There is a good agreement between all parameters. The main differences are the better values based on the ROTAX data (approximatly one order of magnitude). Especially the isotropic thermal vibration parameters are more likely to be correct than the other because of the smaller d-spacing limit in the TOF measurement.

We also took TOF data at the instrument ROTAX of the compound ε-$Fe_3N_{1.25}$. Up to now we have had no success in solving the structure problem in details. We will give more information in future publications.

Table 1: Comparison of results obtained by refinement of neutron (TAS1, Riso) and synchrotron (PD, HASYLAB) diffraction data [6] with results of refinement of TOF data (ROTAX, ISIS) of ζ-Fe_2N

	TAS1 + PD	ROTAX
No. of reflections	28 / 40	160
R_{Bragg} (synchr.) / %	5.6	-
R_{Bragg} (neutron) / %	4.3	4.0
Cell parameters		
a / Å	4.4373(2)	4.4284(2)
b / Å	5.5413(1)	5.5323(2)
c / Å	4.8429(1)	4.8323(2)
Fe on site 8d		
x	0.251(1)	0.2522(5)
y	0.128(1)	0.1210(8)
z	0.0827(6)	0.0824(5)
B(Fe) / Å^2	0.64(8)	1.10(4)
N on site 4c		
x	0	0
y	0.864(2)	0.8648(5)
z	1/4	1/4
B(N) / Å^2	0.0(3)	1.01(6)
occupation factor N	0.94(3)	0.945(7)

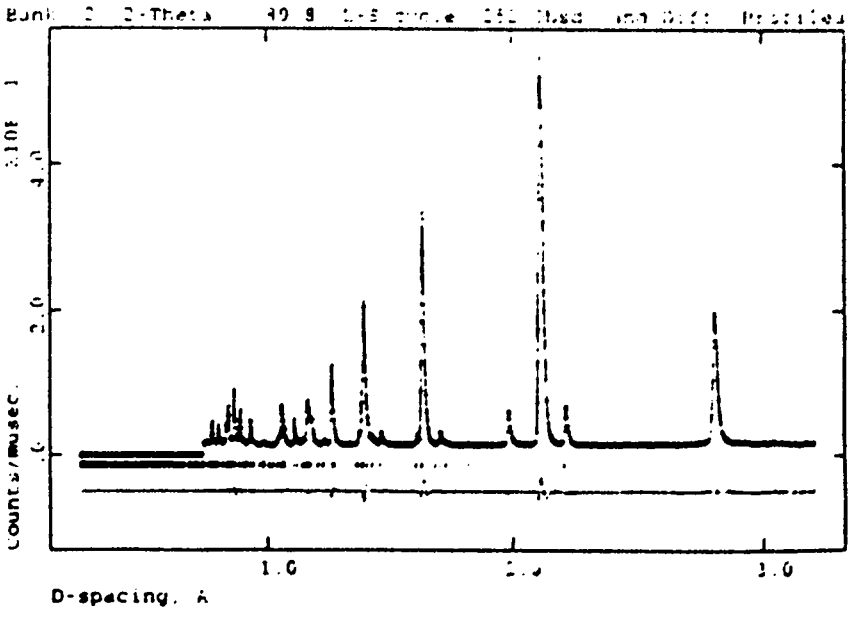

Figure 1: Neutron diffraction diagram (TOF) of ζ-Fe_2N measured at room temperature at ROTAX (ISIS). Dotted curves give measured, full lines calculated values. A difference curve is shown below. The positions of the reflections (vertical signs) are given. An excluded region is marked.

References:

[1] B. Prenosil, Harterei-Tech. Mitt. (HTM) 28 (1973) 157
[2] H. Jacobs, D. Rechenbach and U. Zachwieja, HTM, 50 (1995) 205
[3] K.H. Jack, Proc. Roy. Soc. A 195 (1948) 34
[4] K.H. Jack, Acta Cryst. 3 (1950) 392
[5] K.H. Jack, Acta Cryst. 5 (1952) 404
[6] H. Jacobs, D. Rechenbach and U. Zachwieja, J. Alloys Comp., 227 (1995) 10
[7] D. Rechenbach and H. Jacobs, J. Alloys Comp., in press
[8] D. Rechenbach, Thesis, University of Dortmund 1995
[9] J.K. Cockcroft, Birkbeck College London (UK), Program PROFIL, Version 5.02
[10] A. Larson & R.B. Von Dreele, Los Alamos National Laboratory (USA), Program GSAS 1995

ISIS Experimental Report
Rutherford Appleton Laboratory

RB Number:

Date of Report: march 1996

Title of Experiment: **Orientational disorder in potassium amide KND_2**

Local Contact: W. Kockelmann

Principal Proposer: M. Müller, W. Press — Institut für Experimentalphysik, Universität Kiel
J. Senker, H. Jacobs — Anorganische Chemie, Universität Dortmund
Affiliation:

Instrument: ROTAX / DIFF

Experimental Team: W. Kockelmann, H. Tietze-Jaensch

Date of Experiment: october 1995

Potassium amide KNH_2/KND_2 is an ionic compound. Three phases are known: The high temperature phase ($T \geq$ 348 K [350 K] for KNH_2 [KND_2]) is cubic and of NaCl type, space group $Fm\bar{3}m$. The amide ion NH_2^-/ND_2^- (isoelectronic to H_2O and of similar geometry) is octahedrally coordinated by six potassium cations. It is orientationally disordered because the molecule has $mm2$ symmetry while the site symmetry is $m\bar{3}m$. Potassium amide is tetragonal in a narrow temperature range (348 K[350 K] $\geq T \geq$ 326 K[336 K]). The space group is $P4/nmm$, the site symmetry at the nitrogen position is $4mm$. Thus, the amide group is still displaying orientational disorder. In the monoclinic low temperature phase (space group $P2_1/m$; $T \leq$ 326 K[336 K]) it is further reduced to m. So the NH_2^-/ND_2^- ions are orientationally ordered in this phase.

The diffraction experiment on ROT/DIF was carried out with the deuterated compound KND_2. In the cubic and the tetragonal phase (T = 360 K and T = 340 K, respectively) the scattering angle was $2\Theta = 90°$. In the monoclinic phase complete diffraction patterns (at T = 300 K, 245 K, 200 K, 100 K, 35 K) were obtained by combining measurements at $2\Theta = 37.5°$ and $2\Theta = 119°$.

In both high temperature phases the thermal mean square displacements, especially those of the deuterium atoms, are very large. Thus, higher order reflections get very weak. For the *cubic* phase the number of observable reflections is restricted to seven, and a refinement is almost impossible. The diffraction pattern of the *tetragonal* phase could be used to extract integrated intensities of the reflections. The amide ion can be assumed as a rigid molecular group. The model of PRESS and HÜLLER [1] was used: The deuterium probability density function was expanded into spherical harmonics Y_{lm}. Symmetry adapted functions are all $Y_{l,4\mu}$; in the restricted Q-range, $l_{max} = 4$ is sufficient. Thus, fit parameters are:

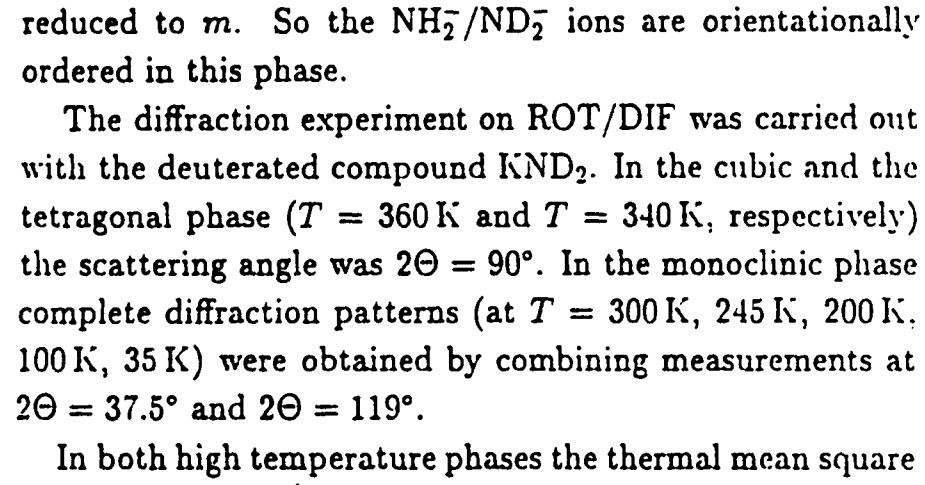

Figure 1: *Deuterium density, as determined in the fits with symmetry adapted functions. Left: cut in (010) plane; right: cut in (001) plane at $z = -0.62$Å (broken line in left picture). The position of the nitrogen is located in the center. Contour lines are plotted equidistantly, all distances are given in Ångström.*

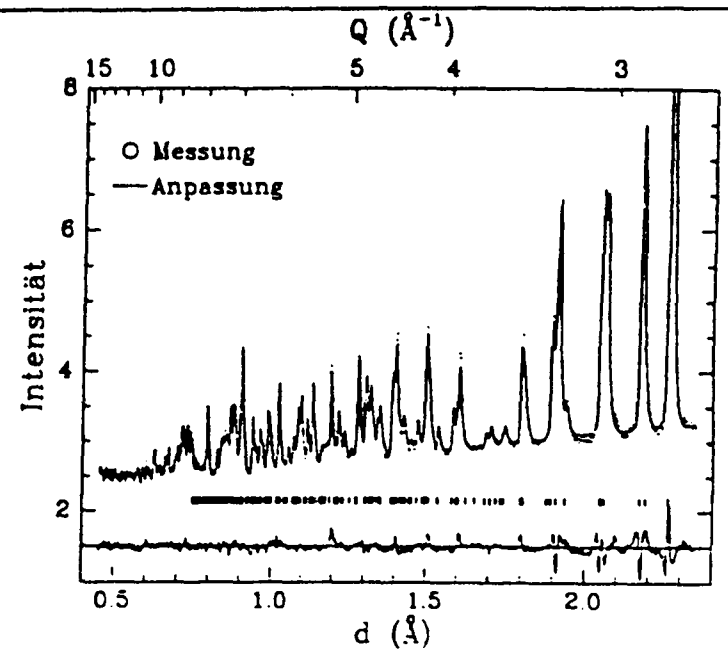

Figure 2: *Rietveld fit to the diffraction pattern of monoclinic KND_2 at T = 35 K, $2\Theta = 119°$. Reflections with $d < 0.75$Å are not marked.*

the 5 coefficients c_{l0} ($l = 1 \ldots 4$) and c_{44}; the mean square displacements and z position parameters of the potassium cation and the rigid amide ion: the N-D distance (radius of the sphere); and a scale factor. Fig. 1 shows the deuterium density as determined in the fit. The amide ion has two equivalent orientations, separated by 90°. There are two hints on rotation-translation coupling: The mean square displacement of potassium is twice as high as that for the amide group, and the radius of the sphere (1.10 Å) is larger than the expected bondlength (1.02 Å). To test models with rotation-translation coupling, single crystal data would be necessary.

The diffraction diagrams of *monoclinic* KND_2 were analyzed using the RIETVELD program GSAS [2]. In Fig. 2 a fit is shown (T = 35 K, $2\Theta = 119°$). A large number of reflections can be observed and separated. The amide ion again was treated as rigid. We used the TLS model (rigid body model) [3] to determine translational and librational thermal displacements. The translational part of the thermal motions shows almost linear temperature dependence, while the libration amplitudes increase strongly towards the phase transition monoclinic-tetragonal. At T = 300 K the libration angles in the plane of the molecular group and around the twofold symmetry axis are $\approx 17°$. Within the TLS model, a correction can be applied to the N-D bondlength. The corrected values (1.03 Å... 1.04 Å) do not differ significantly from the expected bondlength (1.02 Å).

References

[1] W. Press, A. Hüller. Acta Cryst. A 29, 252 (1973)
[2] A. C. Larson, R. B. Von Dreele. Los Alamos National Laboratory (1995)
[3] V. Schomaker, K. Trueblood. Acta Cryst. B 24, 63 (1968)

ISIS Experimental Report
Rutherford Appleton Laboratory

RB Number:

Date of Report: 14th march 1996

Title of Experiment: Structure determination of DPN_2

Local Contact: W. Kockelmann

Principal Proposer: R. Nymwegen, H. Jacobs

Affiliation: Anorganische Chemie I, Universität Dortmund

Experimental Team: W. Kockelmann, H. Tietze-Jaensch

Instrument: ROTAX / DIFF

Date of Experiment: october 1995

HPN_2, known as phospham or as phosphorus(V) nitride imide was first prepared in 1811 by *Davy* [1].

IR-spectroscopic investigations on nearly amourphous material were made by *Goubeau* et al. in 1972. These point to a P-N partial structure analoguous to cristobalite with the hydrogen atoms bonded to nitrogen atoms [2].

The first X-ray diffraction experiments on microcrystalline HPN_2 by *Schnick* et al. in 1991 confirmed these results. The investigations show that the P-N partial structure is built by corner sharing $(P-N_{4/2})^-$ tetrahedra. It was solved in the space group $I\bar{4}2d$ (No 122). A determination of the hydrogen sites was not possible [3].

In our studies we used the high pressure ammonolysis method [4] and succeeded in the preparation of microcrystalline DPN_2.

X-ray powder patterns of this material show one line which is inconsistent with the unit cell given in [3] and four lines indicating lower symmetry. So our diagrams point to a superstructure, probably caused by hydrogen/deuterium or a distorsion of the $(P-N_{4/2})^-$ tetrahedra against each over . A doubling of the c-axis is found.

To get clarity about the exact structure of DPN_2 and to locate the D-atoms we inintiated neutron diffraction experiments with the time of flight method at the ROT/DIFF instrument at ISIS (UK).

The indexing of the reflections extracted from the resulting diffraction diagrams leads to a tetragonal unit cell. This confirms the results of the x-ray powder investigations.

The least square refineiments were carried out with the programm GSAS [5]. We reduced the symmetry of the structure model given in [3] step by step.

It was possible to obtain a proper fit and to achieve an acceptable R-value $\left(R_{Bragg}(F_o^2) = 7{,}6\%\right)$. But by this procedure we did not gain a satisfying solution for the structure up to now. Thus further investigations will be necessary.

It is assumend that the structure of DPN_2 has a tetragonal unit cell but a lower symmetry.

Table 1: Cell parameters for the tetragonal unit cell [pm]

	X-ray diffraction	Neutron diffracttion (ROTT/DIFF)
a	465.22(7)	465.50(5)
c	1411.0(4)	1410.7(4)

Table 2: Indexing of the reflections extracted from the diffraction diagram of the 37° bank

hkl	d (obs.)	d (calc.)	hkl	d (obs.)	d (calc.)
1 0 1	4.420	4.421	1 1 0	3.296	3.293
1 0 2	3.888	3.885	1 1 2	2.987	2.983
0 0 4	3.528	3.527	1 0 4	2.816	2.882

Table 3: Indexing of the reflections extracted from the diffraction diagram of the 119° bank

h k l	d (obs.)	d (calc.)	h k l	d (obs.)	d (calc.)
1 1 4	2.405	2.406	3 1 2	1.440	1.441
2 0 0	2.326	2.327	3 1 3	1.405	1.405
2 0 2	2.209	2.210	3 1 4	1.358	1.358
1 0 6	2.098	2.099	2 1 8	1.345	1.346
2 1 2	1.997	1.997	3 0 6	1.294	1.295
2 0 4	1.942	1.943	3 2 2	1.269	1.270
2 1 4	1.792	1.793	3 1 6	1.247	1.248
0 0 8	1.762	1.763	3 2 4	1.211	1.212
1 0 8	1.648	1.649	2 1 10	1.167	1.168
2 2 2	1.603	1.603	4 0 2	1.148	1.148
2 1 6	1.557	1.559	1 0 12	1.140	1.140
3 0 2	1.516	1.515	3 1 8	1.130	1.130
2 2 4	1.491	1.491	4 1 2	1.114	1.115
3 1 0	1.471	1.472	4 0 4	1.105	1.105

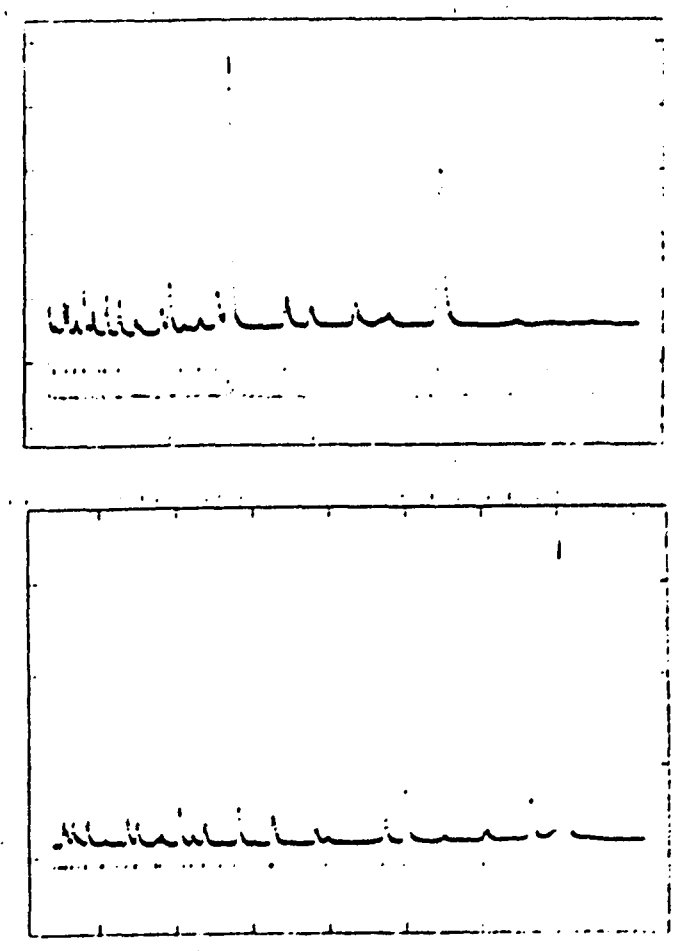

Neutron diffraction digrams of DPN_2 measured at room temperature

References:

[1] E. Steger Chem. Ber., 94, 266 (1961).

[2] J. Goubeau, R. Pantzer Z. anorg. allg. Chem., 390, 25 (1972).

[3] W. Schnick, J. Lücke Z. anorg. allg. Chem., 610, 121 (1992).

[4] H. Jacobs, D. Schmidt Current Topics in Material Science, Vol. 8, 379 (1982), Ed.: E. Kaldis, North Holland Publishing Company.

[5] A. Larson, R. B. von Dreele, Los Alamos National Laboratory (LANL), Program GSAS, 1995.

ISIS Experimental Report
Rutherford Appleton Laboratory

RB Number:

Date of Report: april 1996

Title of Experiment: **Structural study of $Sr(OD,H)_2$**

Local Contact: W. Kockelmann

Principal Proposer: S. Peter, H.D. Lutz

Affiliation: Anorganische Chemie, Universität-GH Siegen

Experimental Team: W. Kockelmann, H. Tietze-Jaensch

Instrument: ROTAX / DIFF

Date of Experiment: october 1995

Structural parameters of the alkali earth hydroxide $Sr(OD,H)_2$ were refined from powder diffraction diagrams taken at 295 K. The sample was deuterated to approximately 80 % corresponding to $Sr(OD_{0.8}H_{0.2})_2$. The hydroxide crystallizes in orthorhombic space group Pnma /1/. The unit cell contains 4 formula units and atoms occupy sites 4c (x, 1/4, z) with D- and H atoms on two crystallographic sites. Recently structural parameters had been obtained by Partin & O'Keefe /2/ for $Sr(OD)_2$ using time-of-flight neutron diffraction data. The aim of the present experiment was to confirm D/H-positions for our sample, to refine thermal parameters and to determine the precise deuterium content.

Data were collected at the ROTAX instrument using JULIOS PSD detectors at a low angle position (2θ=27–57°, d=0.8–10 Å) and a backscattering position (2θ=100–140°, d=0.3–2.3 Å). Diffraction patterns were analysed using the program GSAS /3/. The calculations showed that the structural model as proposed by Partin & O'Keefe /2/ is inconsistent with our data. Refinement of atom positions, isotropic temperature parameters and occupation numbers did not yield acceptible agreement between observed and calculated count rates (fig. 1). A better fit was obtained by admitting anisotropic temperature vibrations u_{ij} (fig. 2, table 1). With anisotropic parameters the peak at 2 Å is fitted more adequately, but there is still disagreement between observed and calculated diagrams. Around 3 Å a diffuse hump hampers a good agreement between observed and calculated profiles. There is possibly a broad range of crystallite sizes causing reflection profile brodening.

Some of the refined temperature parameters are abnormal high, especially u_{11} of O1, D2 and u_{33} of O2, D1 (see table 1). As displayed by the xz-F(obs) Fourier cuts at y=1/4 of fig. 1 and fig. 2 the refinement of anisotropic displacement parameters simulates a smearing of oxygen and hydrogen nuclear densities. We assume that the refined u_{ij} parameters do not represent actual atomic vibrations but result from considerable dynamic or static disorder or a combination of both. The possibility of static disorder at 12 K has already been pointed out by Partin & O'Keefe /2/. Precise atom positions and hydrogen occupation numbers can only be obtained if the disorder is modeled correcty. Analysis of the data is still in progress.

Table 1: Refined structural parameters of $Sr(OD_{0.8}H_{0.2})_2$ at 295 K

lattice parameters: a=9.8627(6) Å b=3.9149(2) Å c=6.1047(6) Å						
	x	z	u11	u22	u33	u13
Sr	0.1620(7)	-0.101(1)	0.041(6)	0.062(7)	0.069(8)	-0.015(6)
O1	0.403(1)	-0.374(1)	0.24(2)	-0.005(5)	0.034(7)	0.006(12)
D1/H1	0.4113(7)	-0.192(2)	-0.001(3)	0.009(5)	0.17(2)	-0.049(8)
O2	0.3820(8)	0.136(2)	0.002(5)	0.056(6)	0.085(15)	0.013(7)
D2/H2	0.464(2)	0.128(2)	0.15(2)	0.039(7)	-0.005(4)	0.060(7)
R_{wp}: 4.6 % R_{Bragg}: 13.3 % (119 deg) 9.8 % (37 deg)						

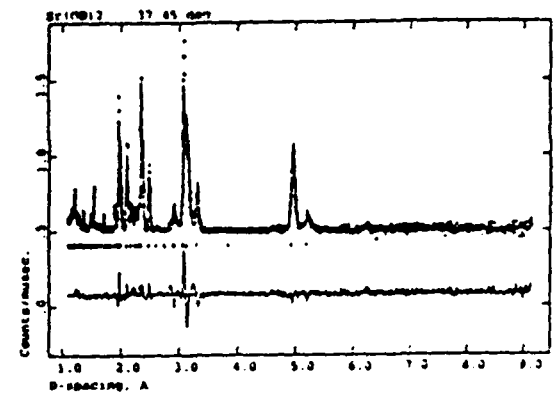

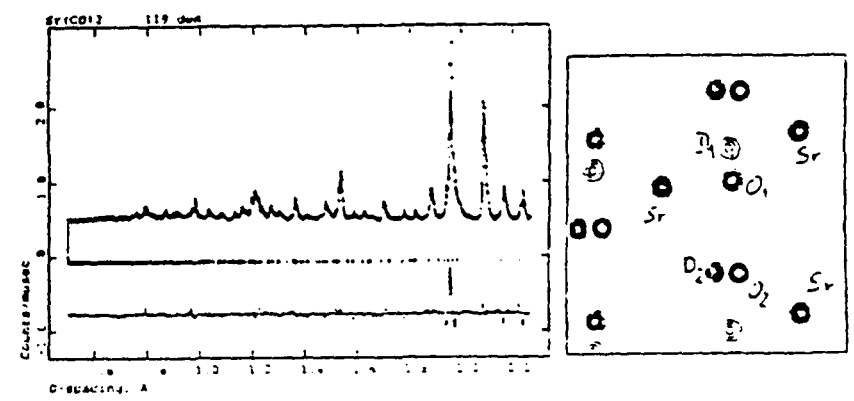

Fig. 1: Left: Rietveld analysis of $Sr(OD,H)_2$ diagrams using isotropic atomic displacement parameters.
Right: 10x10 Å F(obs)-Fourier cut at y=1/4. The origin of the unit cell is at the center of the diagram.

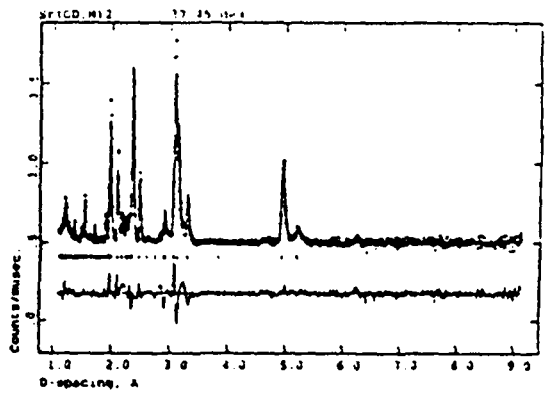

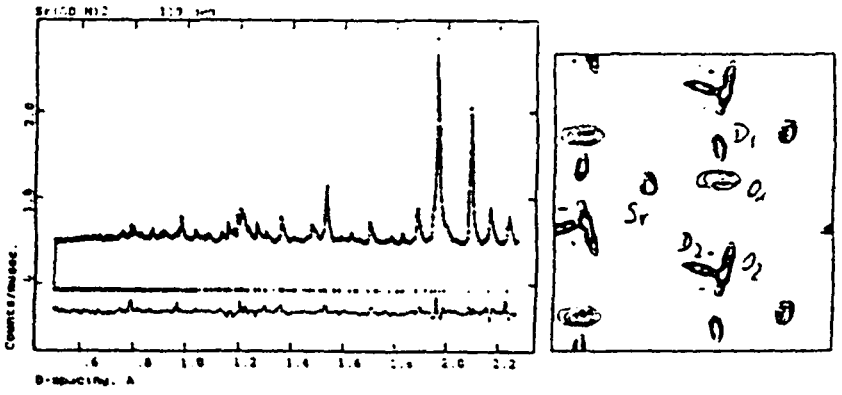

Fig. 2: Left: Rietveld analysis of $Sr(OD,H)_2$ diagrams using anisotropic atomic displacement parameters.
Right: 10x10 Å F(obs)-Fourier cut at y=1/4

/1/ H.W. Grüninger, Dissertation Karlsruhe (1972)

/2/ D.E. Partin and M.O O'Keefe, J. Solid State Chem. 119 (1995) 157

/3/ A.C. Larson and R.B Von Dreele, Los Alamos National Laboratory, General Structure Analysis System - GSAS

ISIS Experimental Report
Rutherford Appleton Laboratory

RB Number:

Date of Report: april 1996

Title of Experiment: Structure refinement of willemite Zn_2SiO_4

Local Contact: W. Kockelmann

Principal Proposer: W. Potzel, Physik Department E15, TU München
E. Rönsch, Institut für anorganische Chemie, TU Dresden

Affiliation:

Experimental Team: W. Kockelmann, H. Tietze-Jaensch

Instrument: ROTAX / DIFF

Date of Experiment: december 1995

The zinc silicate willemite Zn_2SiO_4 crystallizes in the trigonal phenakite structure type in space group $R\bar{3}$. The structure of willemite was proposed /1/ and refined /2,3/ using single crystal X-ray data. The interest on willemite arises from the investigation of magnetic properties in the limited solution series $Fe_{2-x}Zn_xSiO_4$ /4/ in which willemite forms the x=2 endmember. In order to determine precise structural parameters a sample of willemite has been investigated at room and at liquid nitrogen temperatures using neutron diffraction.

A powdered sample of synthetic willemite has been used for the study. The material was prepared by standard solid state reaction of mixed oxide powders. Data sets were recorded on ROTAX at 70 K and 295 K using two JULIOS detectors positioned at a sample–detector distance of 1134 mm and at 2θ-angles of 37.45° and 124.5° respectively. A crystallographic d-spacing range 0.3–10 Å was covered. Fig. 1 shows the diffraction diagrams collected at 295 K as analysed with the GSAS-Rietveld program /5/. Refined parameters are given in table 1. The crystal structure of willemite is displayed in fig 2.

/1/ W.L. Bragg and W.H. Zachariasen, Z. Krist 72 (1930) 518
/2/ Chin'Hang, M.A. Simonov & N.V. Bellov, Sov. Phys. Crystallogr 15 (1970) 387
/3/ K.H. Klaska, J.C. Eck and D. Pohl, Acta Cryst B34 (1978) 3324
/4/ T. Ericson, A.Filippidis, American Mineralogist 71 (1986) 1502
/5/ A.C. Larson and R.B. Von Dreele, Los Alamos National Laboratory, General Structure Analysis System - GSAS

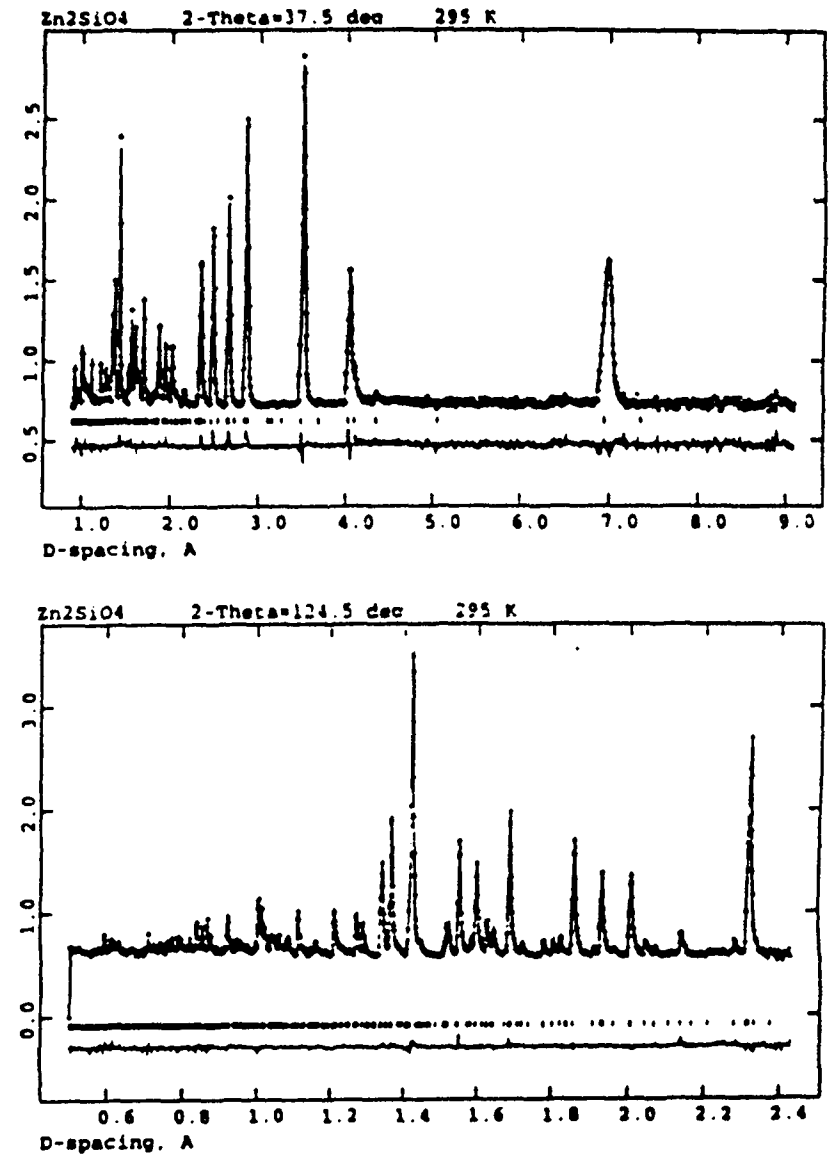

Fig. 1: Room temperature diffraction diagrams of Zn_2SiO_4 taken at detector positions of 37.45° (above) and 124.5° (below).

Table 1: Structural parameters of Zn_2SiO_4 as determined from neutron powder diffraction and single crystal X-ray diffraction /3/.

ROTAX					X-ray		
a=13.9372(2) Å					a=13.948 Å		
c= 9.3100(3) Å					c= 9.315 Å		
	x	y	z	B	x	y	z
ZN(1)	0.9845(6)	0.1925(5)	0.419(3)	0.42(5)	0.98257(4)	0.19167(4)	0.41535(5)
ZN(2)	0.9757(5)	0.1913(6)	0.082(4)	0.42	0.97694(4)	0.19197(4)	0.08140(5)
Si	0.9850(7)	0.1952(6)	0.750(4)	0.6(1)	0.98393(8)	0.19557(8)	0.7494(1)
O(1)	0.1109(4)	0.2162(5)	0.748(1)	0.66(4)	0.1104(2)	0.2164(2)	0.7505(3)
O(2)	0.9957(6)	0.3163(4)	0.750(2)	0.66	0.9958(2)	0.3178(2)	0.7490(3)
O(3)	0.9177(6)	0.1264(6)	0.8945(9)	0.66	0.9164(2)	0.1256(2)	0.8926(3)
O(4)	0.9239(6)	0.1269(6)	0.6052(8)	0.66	0.9227(2)	0.1283(2)	0.6036(3)
R_{wp} = 2.6 % R_B = 3.7 %							

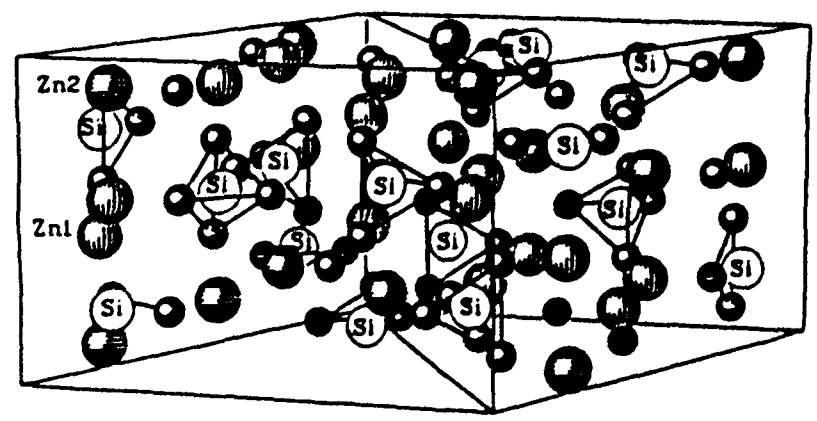

Fig. 2: Unit cell of Zn_2SiO_4

ISIS Experimental Report
Rutherford Appleton Laboratory

RB Number:

Date of Report: march 1996

Title of Experiment: **Structure determination on $KTaN_2$**

Local Contact: W. Kockelmann

Principal Proposer: H. Stegen, H. Jacobs

Affiliation: Anorganische Chemie I, Universität Dortmund

Experimental Team: W. Kockelmann, H. Tietze-Jaensch

Instrument: ROTAX / DIFF

Date of Experiment: july 1995

Potassium nitrido tantalate(V), $K[TaN_2]$

In the last years the interest in ternary nitrides has grown rapidly. In 1988 V. PINKOWSKI synthesized the alkali nitrido tantalates(V), $A[TaN_2]$ (A = Na, K, Rb, Cs) [1].

$Na[TaN_2]$ crystallizes in the α-$Na[FeO_2]$-type and was found to be a quite good conductor for Na^+-ions [2].
$Cs[TaN_2]$ crystallizes in the filled up β-Cristobalite-type. Cs^+-ions are in Friauf-polyhedra [1], CN=12 by Nitrogen.

The structures of $K[TaN_2]$ and $Rb[TaN_2]$ are closely related to that of $Cs[TaN_2]$, but distorted. Both crystallize orthorhombic ($K[TaN_2]$: a = 5.886(1) Å, b = 11.849(2) Å, c = 16.592(4) Å [3]; $Rb[TaN_2]$: a = 6.052(2) Å, b = 12.103(5) Å, c = 17.016(7) Å [1]).
Potassium oxo gallate is isostructural, but hitherto it was not possible to refine the structures of neither $K[TaN_2]$ nor $Rb[TaN_2]$ by using the oxogallate structure model.

To determine the structure of $K[TaN_2]$ an X-ray powder diffraction pattern was obtained. However, the results were not satisfactory, for the Nitrogen position could not be refined beside that of Tantalum.

To overcome this problem neutron diffraction investigations at the ROT/DIF were undertaken. The detector was set at 2θ = 37,45° respectively 89,93°.

To characterize the structure of $K[TaN_2]$, the structural parameters of $K[GaO_2]$ were taken and a refinement was tried with the program GSAS [4].
Unfortunately, the calculated solution is not satisfactory.

The tetrahedra around the tantalum atoms are strongly distorted, the Ta-N-distances reach from 1.79 Å to 2.12 Å - a fact that cannot be explained in a three-dimensional network.
Thus the solution seems to be slightly incorrect, probably because of wrong symmetry. Further investigations to evaluate the right spacegroup for a proper solution of this problem are in progress.

The alkali nitrido tantalates were synthesized at temperatures between 500 °C and 700 °C. At 500 °C $K[TaN_2]$ undergoes a phase transition. This may be the reason why the product is only poorly crystallized. The diffraction pattern cannot be indexed without problems and the right spacegroup could not be found until now.

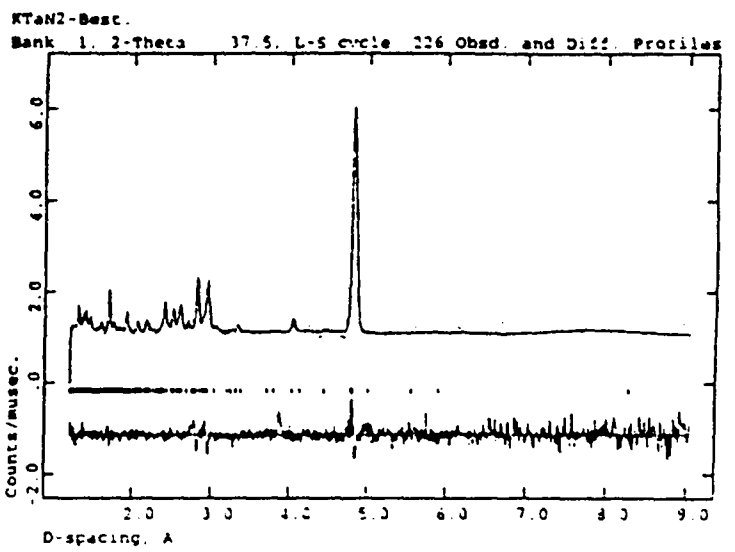

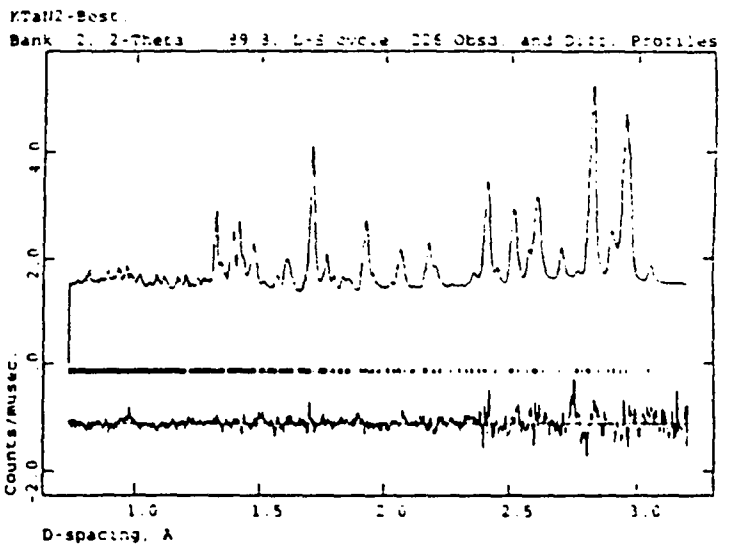

References

[1] *Jacobs, H.; von Pinkowski, E.: „Synthese ternärer Nitride von Alkalimetallen: Verbindungen mit Tantal, $MTaN_2$ mit M Na, K, Rb, Cs"*
J. Less-Common Met. 146 (1989) 147.

[2] *Hellmann, B.; „Synthese und Charakterisierung von Verbindungen $MNbN_2$ mit M = Na, K, Cs. Untersuchungen zur Ionenleitung in $NaTaN_2$; Impedanzspektroskopie an Nitriden"*
Thesis, University of Dortmund 1994.

[3] *Stegen, H.; „Untersuchungen an den Systemen Alkalimetall / Tantal / Stickstoff"*
Diploma, University of Dortmund 1995.

[4] *Larson, A.C.; von Dreele, R.B.; „General Structure Analysis System - GSAS"*
University of California, Los Alamos, 1994.

ISIS Experimental Report
Rutherford Appleton Laboratory

RB Number:

Date of Report: 28 March 1996

Title of Experiment:	Site exchange in novel Rare-Earth Intermetllics	**Local Contact:**	W. Kockelmann
Principal Proposer:	O. Moze	**Instrument:**	ROTAX
Affiliation:	Physics Department, Parma University		
Experimental Team:	W. Kockelmann	**Date of Experiment:**	Oct 1995

Site exchange and magnetic ordering were investigated in a series of novel intermetallics of fundamental and technological interest. These were originally scheduled on POLARIS but sample availability and size meant that measurements were performed on the ROTAX diffractometer after the scheduled POLARIS experiment (RB 6607) when samples of sufficient size were available. The systems studied on ROTAX at room temperature were;

------ $CeNi_3Cu_3$ and $CeNi_4Cu_2$, a possible valence fluctuation system. The structures are variants of the $TbCu_7$ structure (a defect $CeCo_5$ structure, see figure 1). The excellent data set even allowed a refinement of the Ni-Cu distribution on the respective dumbbell sites, Co_{III} and Co_{IV}). The refined data with this structural model is shown in figure. 2). Sample sizes were approximately 1.5 cm^3 and typical counting times were 12 hours.

------ $LaFe_{11}Al_2$ and $LaFe_{11}Al_2N_3$-site occupation and magnetic moments in nitrided cubic Fe-Al RE intermetallics. The pure compound is paramagnetic at room temperature and the refinement clearly shows that Al atoms prefer the 96i site of the cubic $NaZn_{13}$ structure (Z=8, Na at 8a (1/4,1/4,1/4) and Zn at 8b (0,0,0) and 96i (0, 0.18, 0.12). The nitrided compound is strongly ferromagnetic at room temperature due to a 3% expansion of the unit cell from 11.620Å to 11.955Å upon nitridization and a large amount of magnetic scattering was observed in the low angle bank data. The N atoms appear to enter a 2d (0,1/4,1/4) interstitial site. Sample sizes were rather small ($0.3cm^3$) and counting times were 18 hours. Refinement of the magnetic structure is nearing completion.

These experiments clearly demonstrate the extreme utility of ROTAX as an excellent powder diffractometer for magnetic and structural studies. Large backgrounds were a problem for these eperients but measures to suppress the background with the introduction of an evacuated sample tank will largely eliminate this principle obstacle.

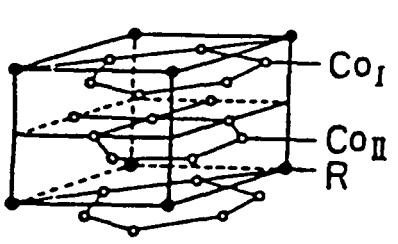

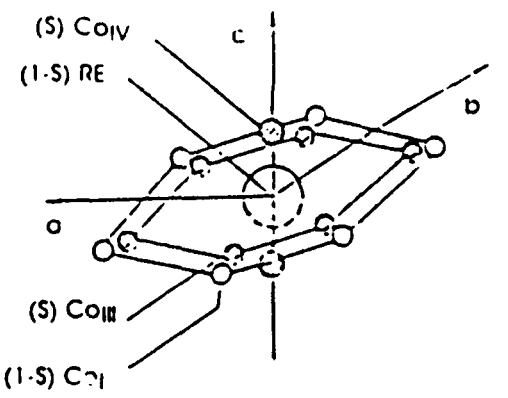

Figure. 1

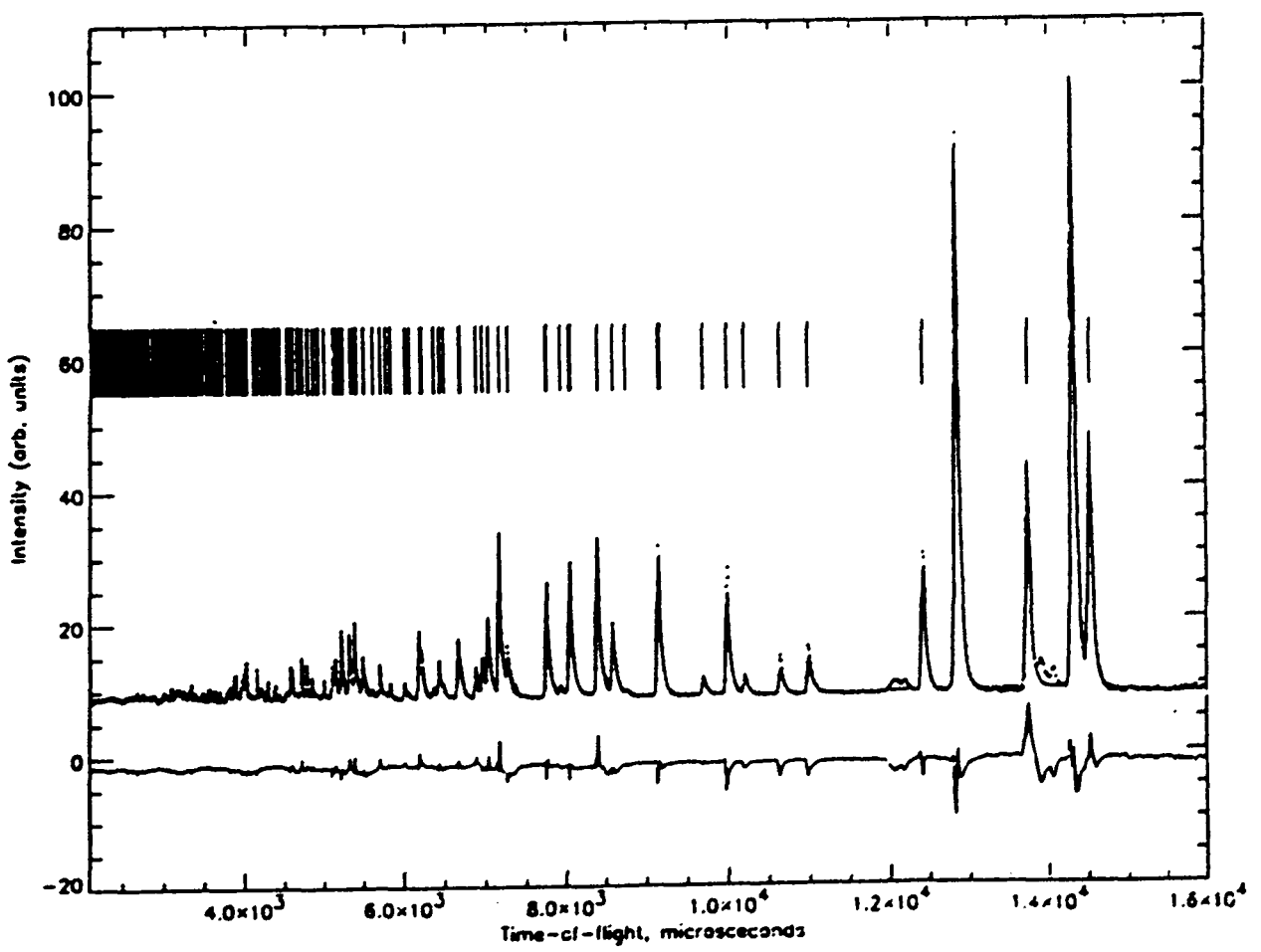

Figure. 2

ISIS Experimental Report

Rutherford Appleton Laboratory

RB Number:

Date of Report: march 1996

Title of Experiment: Structure of Sodium Hexaamidostannate(IV), $Na_2[Sn(ND_2)_6]$

Local Contact: W. Kockelmann

Principal Proposer: F. Flacke, H. Jacobs

Affiliation: Inorganic Chemistry I, University Dortmund

Experimental Team : W. Kockelmann, H. Tietze-Jaensch

Instrument: ROTAX / DIFF

Date of Experiment: october 1995

During the last two years we developed a method of synthesis for hexaamidostannates(IV) of the alkali metals sodium, potassium, rubidium and caesium. We succeeded in growing single crystals of $K_2[Sn(NH_2)_6]$, $Rb_2[Sn(NH_2)_6]$ and $Cs_2[Sn(NH_2)_6]$ and determined their structures by X-ray methods including all hydrogen positions [1]. The powder patterns of the products show only the reflections alkali metal hexaamidostannates(IV). But we were not able to grow crystals of $Na_2[Sn(NH_2)_6]$. From powder patterns we knew that the structures of $Na_2[Sn(NH_2)_6]$ and $K_2[Sn(NH_2)_6]$ must be closely related. So we decided to synthesize a full deuterated sample of $Na_2[Sn(NH_2)_6]$ for structure determination, to compare the D-positions with the H-positions in $K_2[Sn(NH_2)_6]$ and to exclude hydrogen-bridge-bonding in these compounds.

The diffraction measurements were carried out with two positions of a JULIOS detector (37.5°,119°) at 300K for 2d. The neutron powder data were fitted simultaneous with the GSAS package of programs [2] (Fig: 1, 2) to a R_{Bragg}=0.061. The results of the refinements are given in table 1.

Recently we succeeded in growing single crystals of $Na_2[Sn(NH_2)_6]$ and solved the structure by X-ray methods including all hydrogen positions. Now a comparison between results of neutron diffraction on $Na_2[Sn(ND_2)_6]$ with $Na_2[Sn(NH_2)_6]$ and $K_2[Sn(NH_2)_6]$ is possible:

The structure of $Na_2[Sn(ND_2)_6]$ is isotypic with the structure of $Na_2[Sn(NH_2)_6]$ which is closely related to $K_2[Sn(NH_2)_6]$ [1]. They can be described by a cubic close packing of isolated octahedral $[Sn(NH_2)_6]^{2-}$-units. All tetrahedral voids are occupied by the alkali metals.

The orientation of the H and Datoms in the hexaamidostannates(IV) of sodium and potassium shows a great correspondence. The D atoms have just the same orientation as the H atoms in the non deuterated compounds (Fig. 3, 4) in the coordination polyhedron around Sn.

These measurements ensure that the hydrogen positions in $Na_2[Sn(NH_2)_6]$ and also in $K_2[Sn(NH_2)_6]$ are well determined. Hydrogen-brigde-bonds can be excluded in these compounds.

Table 1: Crystallographic data for $Na_2[Sn(ND_2)_6]$

Spacgroup: R-3 (No. 148), a = 5.9803(1)Å, c = 18.4006(3)Å, Z = 3

	R_P	R_{Bragg}
Bank 37.5°	2.7%	5.2%
Bank 119°	1.5%	6.7%
∅	1.8%	6.1%

Site	Atom	x	y	z	B/Å^2
3a	Sn	0	0	0	0.8(1)
6c	Na	0	0	0.1749(5)	1.9(2)
18f	N	0.2914(5)	0.2807(4)	0.0730(1)	1.09(2)
18f	D(1)	0.2519(5)	0.4087(7)	0.0848(1)	3.82(8)
18f	D(2)	0.4522(7)	0.3847(8)	0.0440(1)	3.72(9)

Atom	U_{11}	U_{22}	U_{33}	U_{12}	U_{13}	U_{23}
D(1)	43(2)	36(2)	64(3)	17(2)	-12(2)	-19(2)
D(2)	49(3)	63(3)	37(2)	26(2)	-3(2)	0(2)

Atomic coordinates, isotropic displacement parameters and anisotropic thermal displacement parameters U_{ij} [*10^{1}Å^2] of $Na_2[Sn(ND_2)_6]$
(standard deviation)

Figure 1: Diffraction of $Na_2[Sn(ND_2)_6]$ at 300K, Bank 37.5°

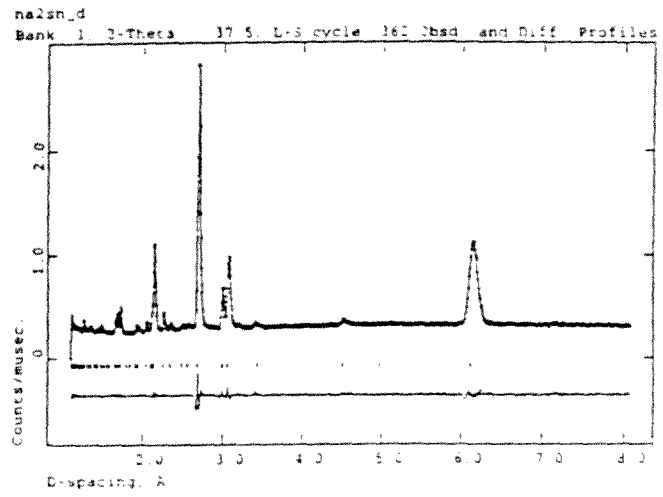

Figure 2: Diffraction of $Na_2[Sn(ND_2)_6]$ at 300K, Bank 119°

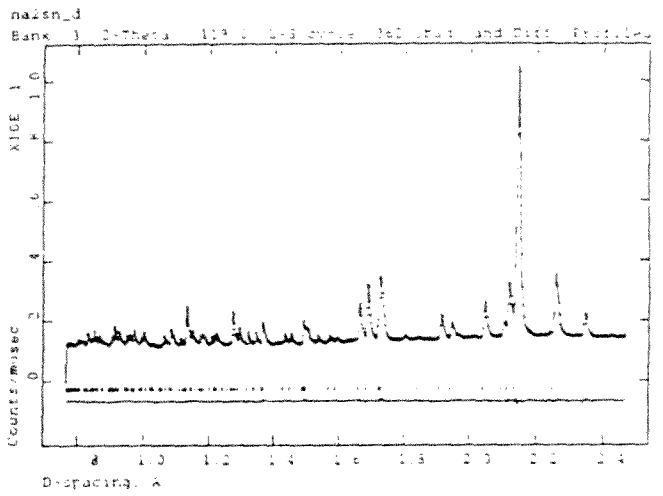

Figure 3: $[Sn(ND_2)_6]^{2-}$-unit of $Na_2[Sn(ND_2)_6]$

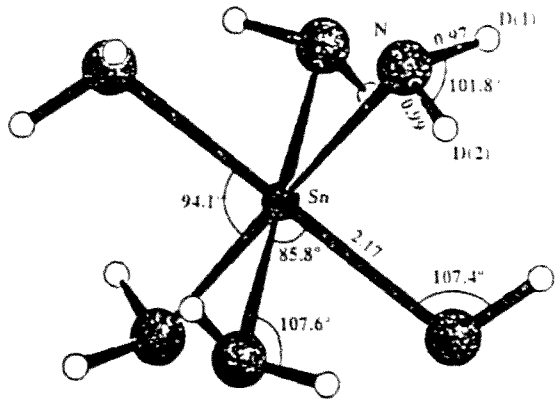

Figure 4: $[Sn(ND_2)_6]^{2-}$-unit of $Na_2[Sn(NH_2)_6]$ with distances and angles of $K_2[Sn(NH_2)_6]$ in brackets

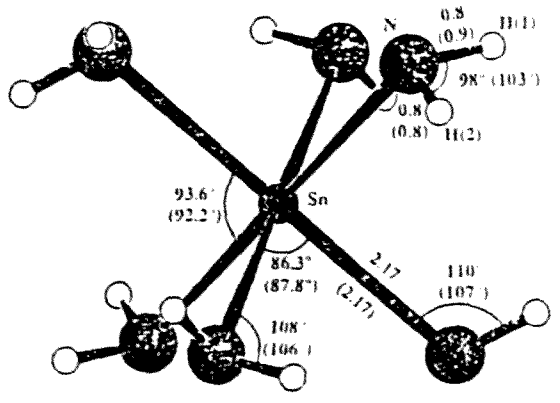

Distances in Å

Literature:

[1] F. Flacke, H. Jacobs, J. Alloys Comp. 227 (1995) 109-115

[2] Al. C. Larson & R. B. von Dreele: Los Alamos Nat. Lab., Los Alamos, NM; Program GSAS General Structure Analysis System; 1994

ISIS Experimental Report

Rutherford Appleton Laboratory

RB Number:

Date of Report: march 1996

Title of Experiment: **Orientational disorder in perovskite related structures of $LiBr*D_2O$ and $Li_2X(OD)$ (X=Cl, Br)**

Principal Proposer: C.Eilbracht and H. Jacobs

Affiliation: Inorganic chemistry I, University Dortmund

Experimental Team : W. Kockelmann, H. Tietze-Jaensch

Local Contact: W. Kockelmann

Instrument: ROTAX / DIFF

Date of Experiment: sept/december 95

We investigated the deuterated samples $Li_2X(OD)$ (X=Cl, Br) and $LiBr*D_2O$ [1] with neutron powder diffraction to get information about the deuteron density in the dynamical/static disordered cubic modifications and to determine the structures of the low temperature modifications. The cubic high temperature modifications of these compounds are closely related to the perovskite structure type of Li_3BrO with partially occupied Li- sites (tab 1).

Tab 1.$CaTiO_3$- related types of structure: space group Pm-3m[

compound		position	
	1b	1a	3d
$CaTiO_3$	Ca	Ti	O
Li_3BrO	Br	O	Li
$Li_2X(OD)$	Cl/ Br	O	Li 2/3
β- $LiBr*H_2O$	Br	O	Li 1/3

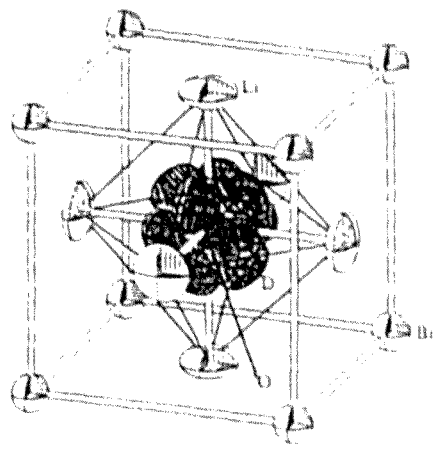

Fig 3: unit cell of the cubic modification of $Li_2Br(OD)$ at T=298 K

For $Li_2Cl(OD)$ and $LiBr*D_2O$ we detected a mainly first order transition from orthorhombic (LT) to cubic (HT) symmetry at T=57 °C/ 32°C by X-ray powder investigations, neutron diffraction [1] and DSC measurements. In the case of $Li_2Br(OD)$ we observed a discontinous behaviour for thermal expansion of the lattice parameter and volume at about 60 °C with preserved cubic symmetry by X-ray and neutron powder investigations.
Solid state ^2H- NMR spectroscopy indicates a dynamical orientational disordering of the hydroxide ions in the high temperature modification of $Li_2Cl(OD)$ and $Li_2Br(OD)$. In the low temperature modification the quadrupol coupling constant (QCC ≅280 kHz) and the asymmetry parameter near zero for both compounds are characteristic for static hydroxide ions.

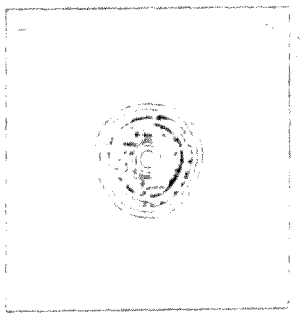

Fig. 1: Fourier cut parallel to the triangular octahedral face of the OLi_6 polyhedra of $LiBr*D_2O$ ([xxx] with x=0.150, T=318 K)

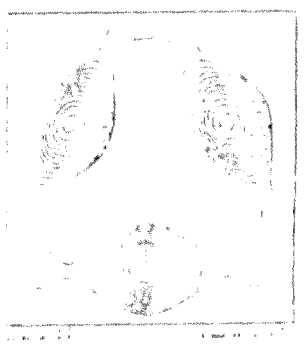

Fig 4: Fourier cut parallel to the triangular octahedral face of the OLi_6 polyhedra of $Li_2Br(OD)$ ([xxx] with x=0.150, T=40K)

The neutron powder diffraction data of cubic $LiBr*D_2O$ (T=318K) fits with an anti $CaTiO_3$ structure type concerning the Li, O, and Br positions. The structure refinements as well as nuclear densities calculated from the observed structure factors support a split model where the deuterons are located towards the octrahedral faces (site 8g) of the Li_6 octahedron (fig. 1, 2). These results are in good agreement with recent neutron powder investigations on $LiBr*D_2O$ which shows larger atomic displacement parallel to the {111} planes at higher temperatures [1].
With a constant wavelength experiment at HMI on $Li_2Cl(OD)$ [1] we have found accumulation of deuteron scattering length density at T=400 K towards the octahedral faces as well. We have investigated the deuterated sample at T=500 K to get information about theevolution of the dynamical disorder of deuterium according to temperature. In the case of higher temperatures the deuteron density distribution seems to be more spherical, so it can not be described with a split model. An analysis of the data using cubic harmonic functions to expand the deuteron scattering length density should lead to a deeper understanding.
The low temperature modifications of $Li_2Cl(OD)$ and $LiBr*D_2O$ show weak superstructure reflections. Because of the only small orthorhombic splitting of reflections the structure determinations are rather difficult and still in progress.

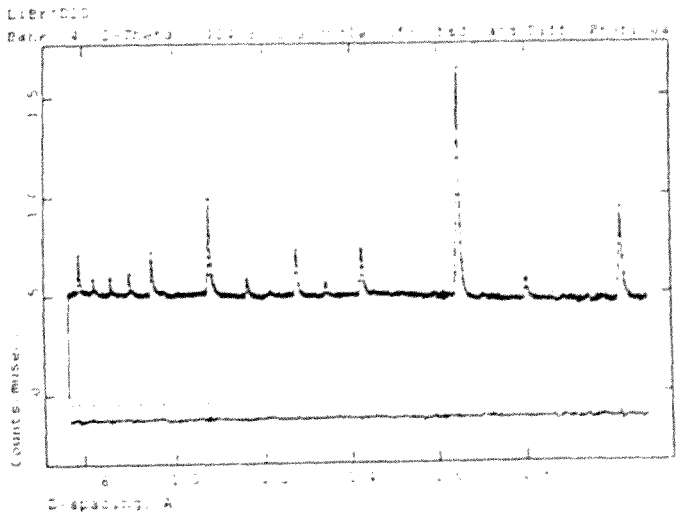

Fig.2: neutron powder diffraction pattern at T=318 K of $LiBr*D_2O$

On $Li_2Br(OD)$ we have carried out neutron powder diffraction measurements at 40 K and 298 K in the LT- and at 420 K in the HT-modification (tab.2, fig. 3,4). In the low temperature modification the deuterium position could be refined on a 12fold site, where the protons of the hydroxide ions are lining up towards the octahedral edges. The above mentioned NMR- investigations and this refinement point out that the hydroxide ions are statically disordered in the [xx0] directions.
Comparing this results with further neutron powder investigations on $Li_2Br(OD)$ the isotropic displacement parameters of Li, Br, and O show no conspicuous increase in the dynamically disordered high temperature phase (tab. 2). The position of deuterium also could be refined on the 12-fold site (12i) as in the LT-modification with a markedly higher Debye- Waller factor. The ^2H- NMR spectra indicate a reorientation process with at least cubic symmetry. Taking into account the results of the neutron powder diffraction a 12-fold- jump process of the deuterons between the octahedral edges is probable.
This process is becoming more and more spherical with increasing temperature. This is the reason why we could not describe the deuteron density with a split model at T= 420K according to the investigations on $Li_2Cl(OD)$.

Tab 2. results of refinement for $Li_2Br(OD)$

	T= 40 K	T= 298 K	T= 330 K	T=370 K
R_I	1.18	1.52	4.25	3.69
R_{II}	5.71	5.92	7.01	7.85
χ^2	9.9	12.0	2.74	2.25
Br	1/2, 1/2, 1/2	1/2, 1/2, 1/2	1/2, 1/2, 1/2	1/2, 1/2, 1/2
O	0.029(1), x, 0	0.032(1), x, 0	0.039(2), x, 0	0.039(2), x, 0
Li	1/2, 0, 0	1/2, 0, 0	1/2, 0, 0	1/2, 0, 0
D	0.134(2), x, 0	0.150(2), x, 0	0.139(3), x, 0	0.139(3), x, 0
$B(Br)/Å^2$	0.55(6)	1.15(1)	1.20(1)	1.56(1)
$B(O)/Å^2$	0.65	1.2*	1.28*	1.68*
$B(Li)/Å^2$	4.1(4)	5.3(3)	4.2(4)	4.0(4)
$B(D)/Å^2$	1.1(1)	5.0(5)	4.5(7)	8(1)
O-D/Å	0.930(1)	0.926(1)	1.00(1)	0.89(1)
instrument restricted	ROT / DIF	ROT / DIF	E2 / HMI	E2 / HMI

[1] BENSC Experimental report 1995
[2] BENSC Experimental report 1994

ISIS Experimental Report

Rutherford Appleton Laboratory

RB Number:

Date of Report: march 1996

Title of Experiment: Orientational disorder in $NaND_2$

Local Contact: W. Kockelmann

Principal Proposer: J. Senker, H. Jacobs — Inorganic chemistry I, University of Dortmund
M. Müller, W. Press — Experimental physics, University of Kiel

Affiliation:

Instrument: ROTAX / DIFF

Experimental Team : W. Kockelmann, H. Tietze-Jaensch

Date of Experiment: december 1995

Former X-ray single crystal and neutron powder diffraction were carried out on $NaND_2$ at room temperature [1]. The structural refinements result in a distorted cubic closed packing of ND_2^- ions. Half of the tetrahedral voids are occupied by Na. Temperature dependent X-ray powder investigations show an unusual behaviour of the lattice parameters (Fig. 1): With increasing temperature the a-axis becomes smaller up to 200 K. At 300 K a change in the gradient of the temperature dependence of the b-axis is observed.

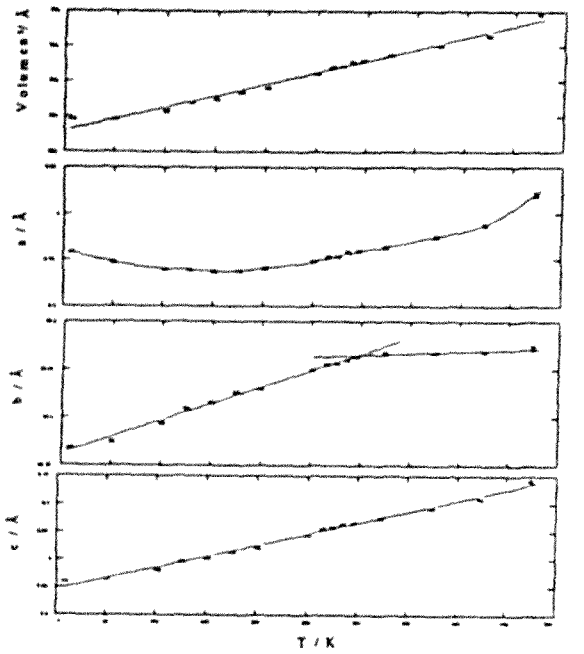

Fig. 1: Temperature dependence of the lattice parameters and the cell volume for $NaND_2$

^{2}H-NMR-data predict a 180° reorientational jump process of the amide ions above 280 K. The jump rates follow an Arrhenius law with a high activation energy of 51 kJ/mol (≈ 520 meV) and τ_0 equal to $5.57 \cdot 10^{13}$ Hz. Furthermore the geometry of fast anisotropic librations of the amide ions was derived from the ^{2}H-NMR measurements. It can be described as a composition of a strongly activated „rocking" libration with weak temperature dependence and a weak „wagging" libration which increases strongly with temperature above 270 K.

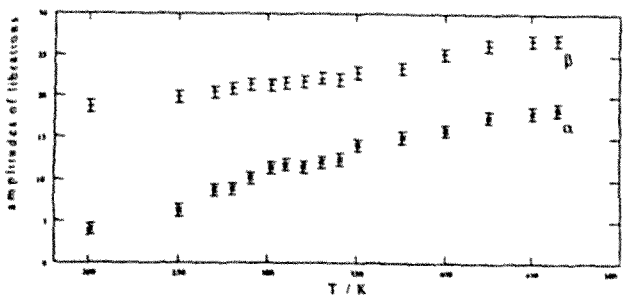

Fig. 2: Temperature dependence of the "rocking"(β) and "wagging"(α) libration for $NaND_2$

However, the amplitudes of the amide ion librations calculated from the NMR data depend strongly on the model of motion used to fit the spectra. Thus it was necessary to check the results with an independent method. For this reason five neutron powder diffraction experiments were carried out on $NaND_2$ in the temperature range between 100 K and 450 K using the instrument ROT/DIF. In order to obtain a large range of d-spacings two positions of the JULIOS detector (2Θ = 37,5°, 124°) were used for each temperature. The observed data were fitted with Rietveld methods [2] using anisotropic displacement parameters for nitrogen and deuterium in the structure model to approximate the displacements due to the amide ion librations. Tab. 1 shows the relevant crystallographic information for the measurement at room temperature. In Fig. 3 a plot of the observed and calculated Rietveld profile fit is depicted.

References

[1] H. Kistrup, H. Jacobs, M. Nagib; Atomkernenergie **26** (1975) 87ff

[2] GSAS; Al. C. Larson, R. B. von Dreele; Los Alamos Laboratory 1994

F d d d (Nr. 70)	x	y	z	B / Å²
16 Na in 16f	7/8	0.0184(3)	7/8	3,8(4)
16 N in 16g	7/8	7/8	0.1119(4)	3.6(3)*
32 D in 32h	0.8322(5)	0.9379(4)	0.1899(4)	8.5(5)*

u / Å²	u_{11}	u_{22}	u_{33}	u_{12}	u_{13}	u_{23}
N	0.041(1)	0.048(2)	0.045(2)	-0.023(2)	0	0
D	0099(4)	0.119(5)	0.099(3)	-0.034(2)	0.035(2)	-0.062(2)

Tab. 1: Results of the refinement for room temperature. Corresponding R_p/R_B values for the refinement is 1.3/5.4 %.

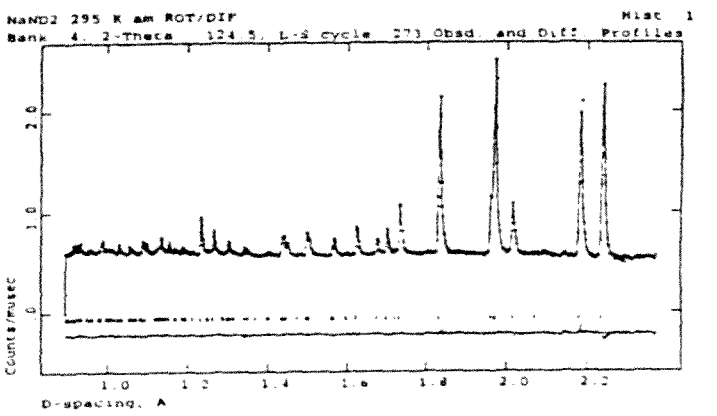

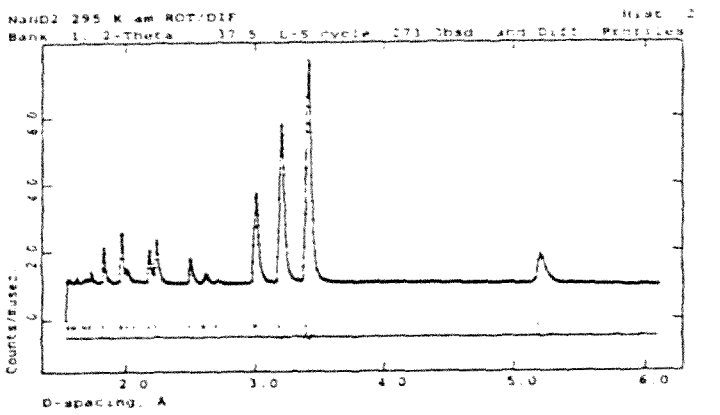

Fig. 3: Rietveld profile fit for NaND2 for room temperature

The results of the neutron powder diffraction experimentes are in good agreement with the thermal expansion and the libration amplitudes of the amide ions determined by NMR spectroscopy. The principal axis r_{yy} of the displacement tensor of D is much larger than the other two axes. r_{yy} represents the displacement in the amide plane and corresponds to the large "rocking" libration determined with NMR spectroscopy. At temperatures above 380 K r_{yy} stagnates which explains the change in the gradient of the thermal expansion of the b-axis. Fig. 4 shows the temperature dependence of the principal axes of the displacement tensor of D.

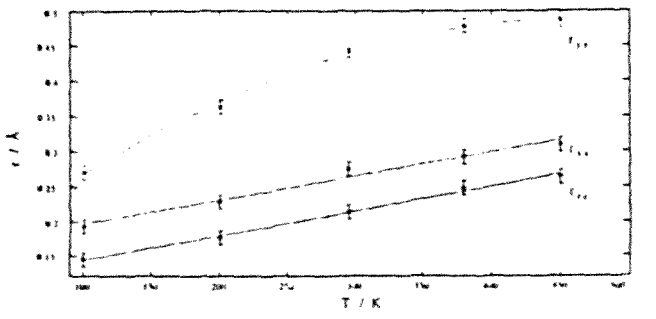

Fig. 4: Principal axes of the displacement tensor of deuterium

For a detailed analysis of the amide ion libration from the thermal displacement parameters of N and D, these values must be treated with a rigid body model to separate the translational and librational components of the thermal displacement parameters. This analysis is still in progress and will be reported later.

ISIS Experimental Report

Rutherford Appleton Laboratory

RB Number: ----------

Date of Report: 21 June 1996

Title of Experiment:	**Domain Distribution and the (B,T) Phase Diagram of Rb_2MnCl_4**	**Local Contact:**	H Tietze-Jaensch
Principal Proposer:	H Tietze-Jaensch	**Instrument:**	**ROTAX /DIFF**
Affiliation:	ISIS. RAL		
Experimental Team:	H Tietze-Jaensch, R v d Kamp, W Kockelmann	**Date of Experiment:**	Jan 1996

1. Introduction

Rb_2MnCl_4 is a quasi 2-dimensional magnetic system that transforms into a uni-axial Ising phase at temperatures below T_N=54 K. Applying an external magnetic field B>5.9 Tesla parallel to the easy c-axis pushes Rb_2MnCl_4 into an xy-like spin-flop phase. Rb_2MnCl_4 crystalizes in the tetragonal K_2NiF_4 structure and forms two degenerated magnetic domains of orthorhombic symmetry Acam or Bbcm upon the para-to-antiferomagnetic phase transition [1].

This experiment on ROTAX was performed to study the domain distribution of a Rb_2MnCl_4 single crystal and to investigate the nature of the phase transitions between the paramagnetic, Ising- and xy-like phases.

2. Experimental

A 1 cm^3 sized Rb_2MnCl_4 crystal with a <100> x <010> orientation was mounted to the 7.5 Tesla vertical cryo-magnet available at ISIS. The temperature and magnetic field dependent integrated intensities of the (1/2 1/2 0) and (-1/2 1/2 0) afm superlattice reflections were studied in tof-diffraction technique at a fixed 2Θ = 37.8 deg scattering angle. The intensity of these Bragg reflections arise from one or the other domain. Their relative volume distribution below T_N is derived from:

$$\frac{I_{D1}(\frac{1}{2}\,\frac{1}{2}\,0) * I_{D2}(-110)}{I_{D2}(-\frac{1}{2}\,\frac{1}{2}\,0) * I_{D1}(110)} = \frac{V(D1)}{V(D2)}$$

Likewise the phasediagram can be plotted from the (1/2 1/2 0) Bragg intensities vs. temperature and external magnetic field B.

3. Results

Fig. 1 shows the domain volume distribution in the Ising and xy phases. It became clear that a Rb_2MnCl_4 crystal forms two magntic domains of equal volumes when driven from the para-magnetic phase into either afm phases, Ising of xy-like phase. Upon isothermal spin-flop transition Rb_2MnCl_4 converts into a mono-domain specimen, regardless whether it is driven from the Ising into the xy-like phase or vice vera. The individual grain sizes in the equi-domain states must be very small, because the Bragg peak widths are considerably broadened in this state, whereas in the mono-domain state the peak widths are entirely resolution determined as are the widths of the nuclear Bragg peaks, like (110), too.

The phase diagram (fig. 2) is derived from the afm Bragg peak intensities. Constant-field and constant temperature scans were performed in the proximity of the triple point of the phases. Together with additional data from the E1 triple axis instrument at HMI Berlin [2] we eventually concluded that the phase diagram is more like a bicritical one as predicted by renormalisation group theory. However, this is in contrast with previous reports by Rauh et al [3] who claimed a "lamda-like" behaviour.

4. Conclusion

In essence we can say that the domain volume distrubtion was determined clearly and undoubtfully. Here, ToF technique proved to be very advantageous for rapidly conducting the simlutaneous measurements of the afm superlattice peaks and their nuclear counterparts at numerous steps in the (B,T) phase diagram of Rb_2MnCl_4. Whereas the academic question about the nature of the phase transitions in proximity to the triple point tangles with the interpretation/interpolation of the direction of the phase boundaries between the experimental scans.

References

[1] G Münninghoff, Ph D Thesis, Uni Marburg, 1980

[2] R v d Kamp et al, HMI report, to be publ.

[3] H Rauh et al, J Phys C 19 (1986) 4503

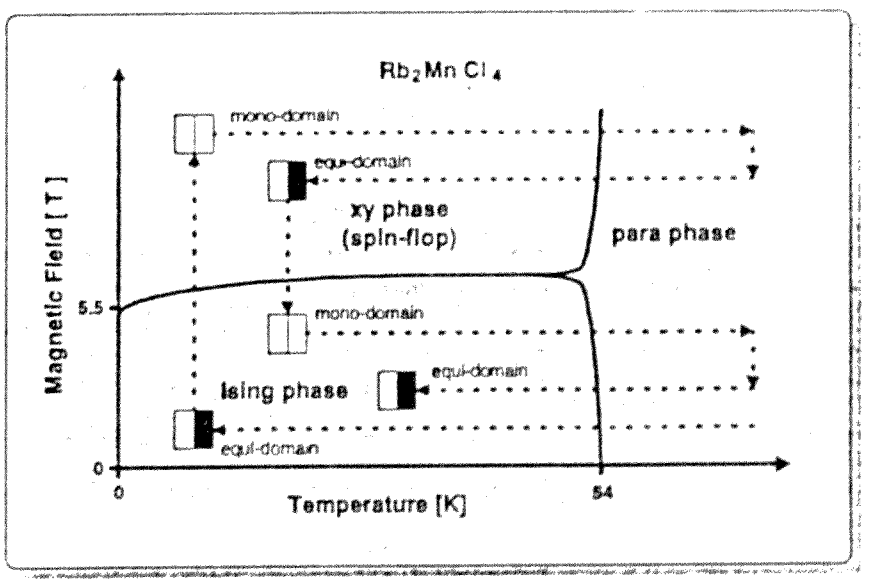

Fig.1: domain volume distribution of Rb_2MnCl_4

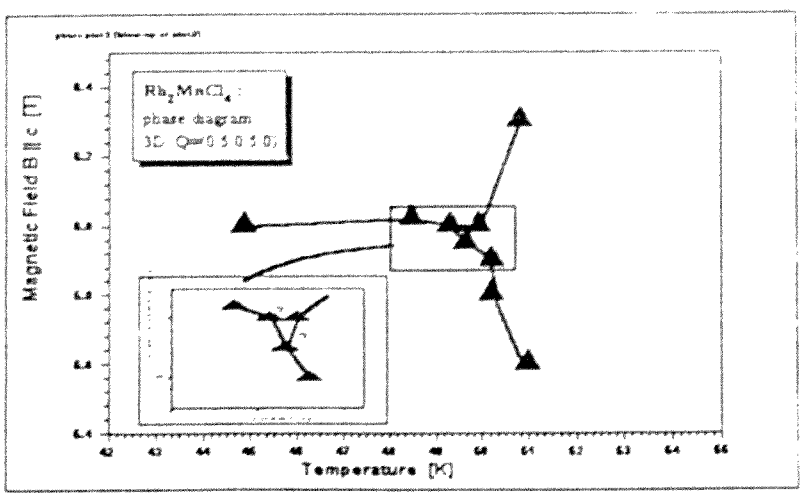

Fig.2: (B,T) phase diagram of Rb_2MnCl_4

ISIS Experimental Report
Rutherford Appleton Laboratory

RB Number: -

Date of Report: may 1996

Title of Experiment: Cation distribution in the spinel compound $Zn_{0.5}LiTi_{1.5}O_4$

Local Contact: W. Kockelmann

Principal Proposer: W. Potzel, Physik Department E15, TU München
E. Rönsch, Institut für anorganische Chemie, TU Dresden
Affiliation: W. Schäfer, Mineralogisches Institut, U Bonn

Experimental Team: W. Kockelmann, H. Tietze-Jaensch

Instrument: ROTAX / DIFF

Date of Experiment: november 1995

Oxide spinels exhibit a large variety of electronic and magnetic properties. Some spinels like $LiTi_2O_4$ are superconductors with a relatively high transition temperature /1/. The magnetic properties of iron containing spinels like $ZnFe_2O_4$ /2/ are of special interest with respect to magnetic storage devices and other technological applications. Normal oxide spinels are described by the formula $(A)[B_2]O_4$ where A and B refer to tetrahedral and octahedral sites, respectively. The other basic type is the inverse spinel $(B)[AB]O_4$, where divalent A ions and half of the trivalent B ions have changed sites. Typical normal spinels are $(Zn)[Fe_2]O_4$ and $(Zn)[Al_2]O_4$, whereas $(Zn)[ZnTi]O_4$ is an example of an inverse spinel. The properties of Zn and Fe containing spinels have been extensively studied by Mössbauer spectroscopy, μSR measurements and neutron diffraction /2-4/.

Spinel compounds of the composition $Zn_{0.5}LiTi_{1.5}O_4$ were now investigated by means of neutron powder diffraction in order to refine crystal structure parameters. The particular aim was to derive the cation distribution on tetrahedral and octahedral sites, respectively. Three powdered samples of $Zn_{0.5}LiTi_{1.5}O_4$ were produced from corresponding metal oxides. Two of them were processed using conventional techniques with preparation temperatures up to 1100°C, using metal oxides in stoichiometric amounts (P1=product 1) and 3 % extra Li_2O oxide (P2=product 2), respectively. For a third compound preparation temperatures had always been below 800°C using a 3 % surplus of Li_2O oxide (P3=product 3). Powder diffraction diagrams were collected at room temperature on ROTAX/DIFF using two JULIOS detector units centered at 2θ=37.45° and 124.5°, respectively.

Sections of the diffraction diagrams of the three specimen P1, P2 and P3 are shown in fig. 1. A striking difference between the three curves is, that peak/background ratios in P1-diagrams are smaller by a factor of 3 compared to diagrams of samples P2 and P3. The diffraction patterns of all samples show small superlattice reflections in addition to reflections of the normal (or inverse) spinel structure type (space group Fd3m), ruling out a total statistical distribution of cations. An order on A-site, described in space group $P2_13$, can be ignored in the first place, since no superstructure peak at 4.2 Å is observed. However, the observed superlattice peaks can be explained by an order of ions onto two octahedral sites B' and B'' according to the formula $(A)[B'B'']O_4$ (space group $P4_332$). The program GSAS /5/ was used to carry out the Rietveld refinements (see fig. 2).

The analysis of the powder patterns yields the same preferential site occupation of cations for samples P1, P2 and P3 (see table 1). There is a more or less complete 1:3 order of Li and Ti ions on octahedral B-sites: Li atoms occupy site 4(b), whereas 12(d) is fully occupied with Ti ions. The remaining Zn and Li atoms are randomly distributed on the tetrahedral 8(c) site.

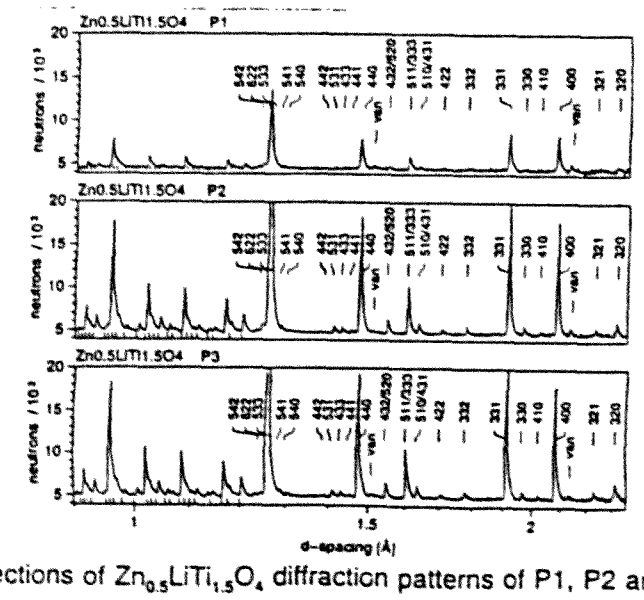

Fig. 1: Sections of $Zn_{0.5}LiTi_{1.5}O_4$ diffraction patterns of P1, P2 and P3.

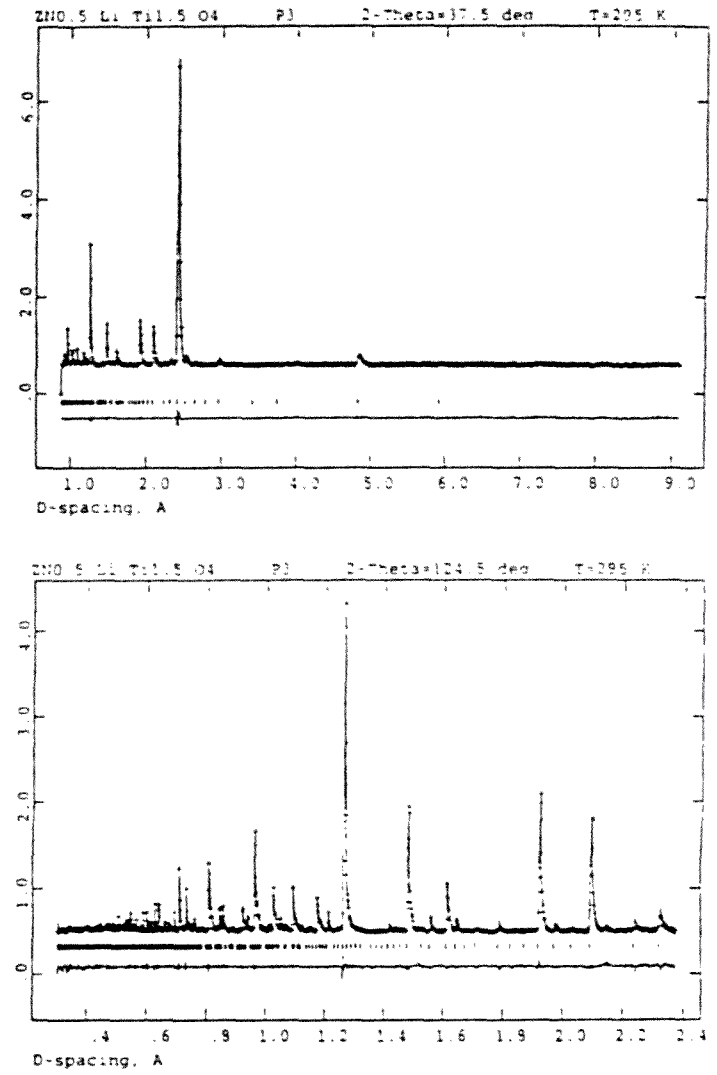

Fig. 2: Profile fit of forward scattering (above) and backscattering (below) patterns of $Zn_{0.5}LiTi_{1.5}O_4$ (P3).

Table 1: Structural parameters of $Zn_{0.5}LiTi_{1.5}O_4$. N values denote occupation numbers in percent. Profile R_{wp} and Bragg-R_B values refer to the forward-/backscattering diagrams, respectively.

$(A)[B'B'']O_4$		P1	P2	P3
lattice parameter:	a [Å]	8.3792(2)	8.3776(1)	8.3791(1)
tetrahedral site 8(c):	x_A	-0.003(3)	-0.001(1)	0.000(1)
	N_A(Zn)	0.493(4)	0.499(2)	0.500(2)
	N_A(Li)	0.507(4)	0.501(2)	0.500(2)
octahedral site 4(b):	$N_{B'}$(Zn)	0.015(8)	0.002(3)	0.00(4)
	$N_{B'}$(Li)	0.985(8)	0.998(3)	1.00(4)
octahedral site 12(d):	$x_{B''}$	0.367(1)	0.3669(4)	0.3664(4)
	$N_{B''}$(Ti)	0.97(2)	1.00(1)	1.00(1)
oxygen site 8(c):	x(O1)	0.3895(8)	0.3896(3)	0.3901(3)
oxygen site 24(e):	x(O2)	0.1422(7)	0.1431(3)	0.1433(3)
	y(O2)	0.8588(6)	0.8592(2)	0.8594(2)
	z(O2)	0.1220(5)	0.1231(2)	0.1226(2)
	B_{av} [Å²]	0.46(5)	0.23(2)	0.25(1)
	R_{wp} [%]	2.6 / 2.2	2.6 / 3.3	3.1 / 3.5
	R_B [%]	9.3 / 12.0	6.5 / 5.2	8.1 / 7.8

/1/ D.C. Johnson, J. Low Temp. Phys. 25 (1976) 145.
/2/ W. Schiessl, W. Potzel, H. Karzel, M. Steiner, G.M. Kalvius, A. Martin, M.K. Krause, I. Halevy, J. Gal, W. Schäfer, G. Will, M. Hillberg, R. Wäppling, Phys. Rev B53 (1996) 9143.
/3/ D.W.Mitchel, T.P. Das, W. Potzel, W. Schiessl, H. Karzel,, M. Steiner, M. Köfferlein, U. Hiller, M. Kalvius, A. Martin, W. Schäfer, G. Will, I. Halevy and J. Gal, Phys. Rev. B53 (1996) 7684.
/4/ W. Potzel, M. Kalvius, W. Schiessl, H. Karzel, M. Steiner, A. Kratzer, A. Martin, M.K. Krause, A. Schneider, I. Halevy and J. Gal, W. Schäfer, G. Will, M. Hillberg, R. Wäppling, D.W.Mitchel and T.P. Das, Hyp. Int. 97 (1996) 373.
/5/ A.C. Larson and R.B. Von Dreele, Los Alamos National Laboratory, General Structure Analysis System - GSAS.

ISIS Experimental Report

Rutherford Appleton Laboratory

RB Number:

Date of Report: april 1996

Title of Experiment: Sinusoidal magnetic structure of $TbCo_{0.5}Ni_{0.5}C_2$

Local Contact:

Principal Proposer: J.K. Yakinthos — Electrical and Computer Engineering Department, Democritos University of Thrace, Greece

Affiliation: W. Kockelmann — Mineralogical Institute of Bonn University

Instrument: ROTAX / DIFF

Experimental Team : W. Kockelmann

Date of Experiment: sept 1995

Ternary compounds RTC_2 (R=heavy rare earth, T=Co, Ni) crystallize isostructurally in the orthorhombic $CeNiC_2$-type structure in space group Amm2 /1/. These 4f-3d intermetallic compounds are of fundamental magnetic interest with respect to the variation of the two different magnetic partners and, consequently, different magnetic interactions within the same crystal structure. The ternary $RCoC_2$ compounds are ferromagnetic whereas the $RNiC_2$ compounds exhibit different types of antiferromagnetic structures /2/. Previous neutron diffraction measurements on the mixed compound $TbCo_{0.5}Ni_{0.5}C_2$ had shown long range magnetic order of Tb moments consisting of a main (in)commensurate sinusoidal component and a second small ferromagnetic component /2/. The temperature behaviour of the magnetic structure of $TbCo_{0.5}Ni_{0.5}C_2$ has now been re-examined in greater detail.

The same material of polycrystailine $TbCo_{0.5}Ni_{0.5}C_2$ as in the previous study was used. The powder was prepared in an arc melting furnace under argon atmosphere. The ingot was remelted several times to achieve homogeneity. Diffraction patterns were recorded on ROTAX at temperatures between 4.5–20 K using JULIOS-PSD detectors at two 2θ-positions covering 2θ-ranges from 5 to 40° and 48 to 86° respectively.

Powder diffraction patterns of $TbCo_{0.5}Ni_{0.5}C_2$, recorded at 4.5 K and 20 K, are shown in fig. 1. Magnetic order manifests itself clearly by the huge magnetic $(000)^{\pm}$-peak at 21 Å. The enormous width of this reflection is due to the relaxed Δd/d-resolution at low scattering angles. The temperature dependence of the integrated intensity of this reflection (fig. 2) indicates a magnetic ordering temperature of about 15 K. Magnetic peaks were indexed with a propagation vector **k**=[0.165(1), 0, 0] =[1/6, 0, 0]. Within experimental errors the propagation vector is commensurate and does not vary with temperature (fig. 2).

Integrated magnetic intensities were extracted from the diffraction diagrams to determine magnetic moment values and directions using the program POWLS /3/. In accordance with previous findings /2/ magnetic intensities can be explained by a transverse sine-modulated structure of Tb moments: The magnetic moment amplitude is $\mu(Tb)=6.7(3)\ \mu_B$ at 4.5 K; moments are aligned parallel to the c-axis. Contrasting previous findings there is no evidence for an additional ferromagnetic Tb moment component. Magnetic moments of Co- and Ni are not ordered. In the inspected temperature regime the magnetic structure remains sinusoidal: there is no evidence of a squaring-up of the magnetic moment distribution towards lower temperatures.

/1/ W. Jeitschko, M.H. Gerss, J. Less-Common Metals 116 (1886) 147

/2/ W. Schäfer, W. Kockelmann, G. Will, J.K. Yakinthos and P.A. Kotsanidis, Zeitschrift für Kristallographie 211 (1996) 106 (and references therein)

/3/ W. Kockelmann, E. Jansen, W. Schäfer and G. Will, reports of Forschungszentrum Jülich Jül-3024 (1995)

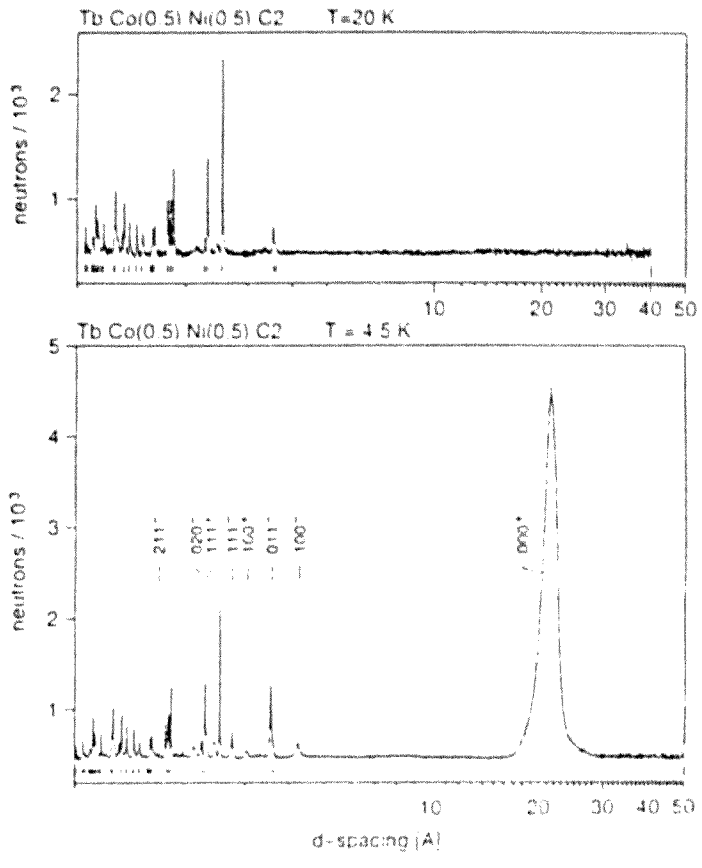

Fig. 1: Diffraction patterns of $TbCo_{0.5}Ni_{0.5}C_2$ at 20 K (above) and 4.5 K (below). Magnetic peaks are indexed according to $(hkl)^{\pm}=(h,k,l)\pm(1/6, 0, 0)$.

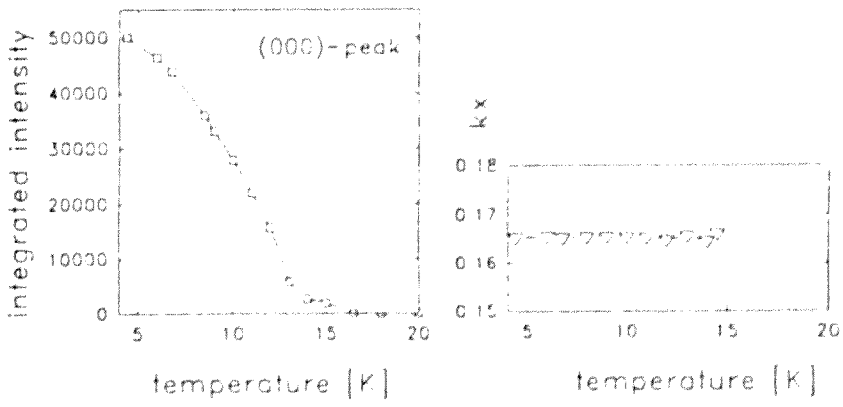

Fig. 2: $(000)^{\pm}$ peak intensity (left) and propagation vector $[k_x, 0, 0]$ (right) as a function of temperature. Error bars are about the size of the symbols.

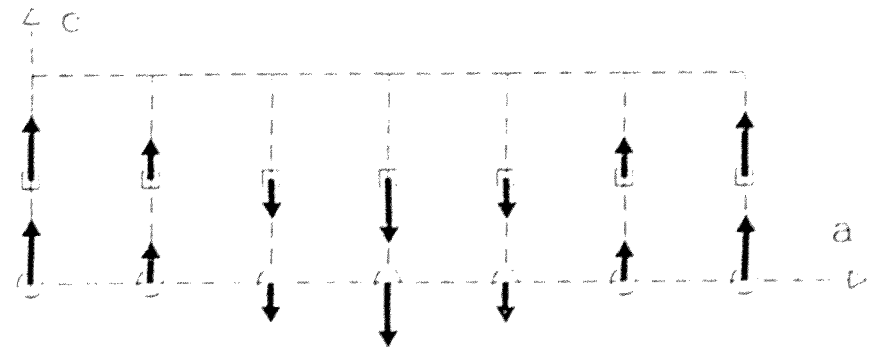

Fig. 3: Schematic representation of the transverse sine-modulation of magnetic Tb-moments in $TbCo_{0.5}Ni_{0.5}C_2$.